



COVID-19 drugs: A critical review of physicochemical properties and removal methods in water

Zihe Chen^a, Jiani Xu^a, Cong Li^{a,*}, Jingzhen Su^a, Yulin Bian^a, Hyunook Kim^b, Jinfeng Lu^c

^a School of Environment and Architecture, University of Shanghai for Science and Technology, Shanghai 200093, China

^b University of Seoul, Department of Environmental Engineering, 163 Seoulsiripdae-ro, Dongdaemun-gu, Seoul 02504, South Korea

^c School of Environmental Science and Engineering, Nankai University, Tianjin 300071, China

ARTICLE INFO

Keywords:

Covid-19 pandemic
Antiviral drugs
Water treatment
Advanced oxidation
Biological treatment

ABSTRACT

In the post-Corona Virus Disease 2019 (COVID-19) era, the presence of COVID-19 drugs in the environment has garnered significant attention. These drugs persist in aquatic environments due to their photostability and biological activity. In Wuhan, China, the concentration of chloroquine in surface water reached 20,00 ng/L during the COVID-19 outbreak [1]. Lopinavir, ritonavir, abacavir, zidovudine, efavirenz, nevirapine, lamivudine, and telbivudine have all been detected in aquatic environments [2,3]. This study provides a comprehensive overview of the physicochemical properties and chemical structures of COVID-19 drugs. It reviews and summarizes the removal techniques for these drugs, including biological methods, advanced oxidation processes, and physical treatment technologies. The concept of "COVID-19 specific drugs" is introduced, highlighting their anticipated long-term use in the treatment of COVID-19. Additionally, this study presents a novel analysis of the removal mechanisms of ferrate for COVID-19 drugs and explores future research directions in wastewater treatment technologies for the post-COVID-19 era.

1. Introduction

In December 2019, COVID-19 outbreak emerged in Wuhan, Hubei Province, China. This was the first global instance of COVID-19. As of 15 June 2024, the cumulative number of COVID-19 cases reported by the World Health Organization globally has reached 775,552,205, with 7010,681 deaths [4]. Among them, the reported cases of infection in the United States and China reached 103 million and 99.4 million respectively [5]. In May 2023, the World Health Organization (WHO) declared that the global emergency it had created was over [6]. COVID-19 is still prevalent around the world, and since the outbreak of COVID-19, the novel coronavirus has continuously mutated over time, producing new variants. Includes the novel coronavirus variant strains *Alpha*, *Beta*, *Gamma*, *Epsilon*, *Zeta*, *Eta*, *Theta*, *Lota*, *Kappa*, *Lambda*, *Mu* and *Delta* [7].

Initially, at the onset of the COVID-19 pandemic, there was no specific treatment for COVID-19. Based on previous clinical experience in the treatment of viral infections, people infected with COVID-19 have been treated with a large number of antiviral drugs, oseltamivir (OP) [8], acyclovir (ACV), ribavirin (RBV), arbidol (ABD) [9], remdesivir (RDV) [10] etc. Antibiotic treatment, amoxicillin (AMX), cephalosporin

(CEP) [11], vancomycin (VAN), doxycycline (DOX) [12] etc. Non-steroidal anti-inflammatory drugs (NSAIDs) treatment, ibuprofen (IBU) [13], chloroquine (CQ) [14], hydroxychloroquine (HCQ) [15], acetaminophen [16]. And traditional Chinese medicine treatment lian-hua qingwen capsule (LQC), huoxiang zhengqi wan (HZW) [17]. These drug treatments have not shown a very significant effect on the fight against COVID-19. With the continuous improvement of human cognition of COVID-19, more drugs have been put into clinical use. Studies have shown that lopinavir (LPV) - ritonavir (RTV) combination has antiviral effects on SARS-CoV-2 [18], azivudine (AZV) and paxlovid (PXVD) have been used clinically in China [19,20]. The results showed that AZV was more effective than PXVD in treating hospitalized COVID-19 patients with existing comorbidities [21]. Arbidol demonstrated statistically significant efficacy in mild asymptomatic patients in a double-blind, placebo-controlled trial [22]. Clinical trials have been conducted in the United States, China, Japan, Korea and other countries. This class of drugs has a significant inhibitory effect on COVID-19, known as the new coronavirus specific drugs (NCSDs).

As shown in Fig. 1, NCSDs are not fully metabolized in the patient's body, and the incomplete metabolized part is excreted from the body in the form of feces and urine, and eventually reaches wastewater

* Corresponding author.

E-mail address: licong@usst.edu.cn (C. Li).

<https://doi.org/10.1016/j.jece.2025.115310>

Received 22 October 2024; Received in revised form 30 December 2024; Accepted 2 January 2025

Available online 3 January 2025

2213-3437/© 2025 Published by Elsevier Ltd.

treatment plant (WWTP) [23]. However, existing wastewater treatment processes are primarily designed for conventional urban wastewater and have not adequately accounted for the increased concentrations of antiviral drugs in influent wastewater, a consequence of the widespread use of antibiotics, immunomodulators, and antiviral medications during the pandemic [2]. The traditional wastewater treatment process of WWTP has limited removal efficiency for new pollutants such as antiviral drugs and antibiotics [3]. For example, sulfamethoxazole (SMZ) has a removal rate of 44 % in WWTP [24]. The highest removal rate of nevirapine (NVP) was 49 % in a WWTP in Kenya [25]. At present, only abacavir (ABC) and lamivudine (3TC) can be completely removed by sewage treatment plants, and the average removal efficiency of other antiviral drugs is less than 70 % [3]. These pollutants have low biodegradability [26]. In traditional water treatment processes, these NCSDs may affect the biological activity of activated sludge during treatment, resulting in fluctuations in effluent water quality, which may lead to substandard effluent water quality. These NCSDs eventually reach natural water bodies. As shown in Table 1 The concentration of ATV in surface water detected in 11 countries in Asia, Europe and Africa has reached the level of ng/L [27]. Such as 3TC (5.43 $\mu\text{g/L}$), NVP (4.86 $\mu\text{g/L}$), zidovudine (ZDV) (7.68 $\mu\text{g/L}$) and amantadine (AMT) (10.30 $\mu\text{g/L}$) [28,29]. Kumar et al. highlight that widespread use of antivirals during the COVID-19 pandemic significantly increases the risk of biological resistance [30]. Some antiviral drugs have also been shown to be toxic to some fish, which persist in aquatic environments for an extended period, resulting in antiviral drug resistance [31,32]. Once the concentration of these drugs in the aquatic environment accumulates to a certain degree, contaminated water flows into waterworks and eventually enters the human body through drinking water, presenting risks and potential threats to human health and ecological environmental safety.

The existing water treatment removal technologies are mainly divided into three categories: chemical method, biological treatment method and physical method. Advanced oxidation method mainly produces reactive oxygen species to attack pollutants and achieve the effect of degrading pollutants. The biological treatment method uses microorganisms to oxidize pollutants by domesticating activated sludge and converting them into harmless substances or small molecules. The adsorption method is to remove the target pollutant by electrostatic attraction or intermolecular force. The removal efficiency of water treatment technology is also very different for different types of NCSDs.

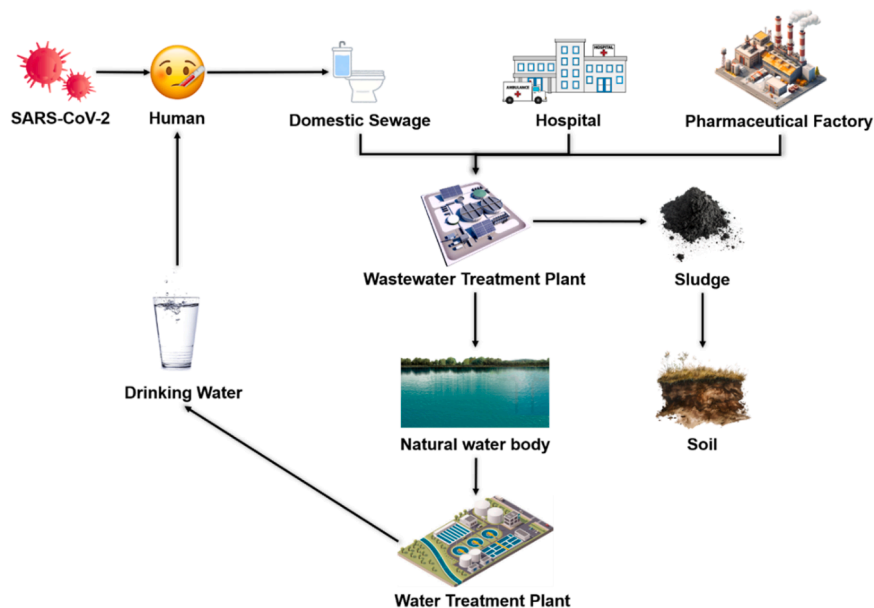
Table 1

The presence of some antiviral drugs in water environments.

Drugs	Concentration (ng/L)	Aqueous matrix	Country	Toxicity Risk
Chloroquine	20000 [1]	Surface water	Wuhan, China	High [33,34]
Dexamethasone	55.6 [35]	Surface water	Hungary	Moderate [36,37]
Favipiravir	64 [38]	Domestic wastewater	Japan	Moderate [39]
Lamivudine	20 [40]	Surface water	Germany	Moderate [41]
Lopinavir	3800 \pm 350 [42]	WWTP Effluents	KwaZulu-Natal, South Africa	Moderate [43]
Ribavirin	10 [44]	WWTP Effluents	Germany	High [45]
Ritonavir	12 \pm 5 [46]	Surface water	France	Moderate [43]

Notes: Toxicity risks are roughly classified according to the severity and probability of occurrence of toxicity.

The octanol-water partition coefficient (K_{ow}) is a widely used physicochemical parameter that describes the distribution behavior of a compound between two immiscible liquids: n-octanol and water. The K_{ow} value reflects the hydrophobicity or lipophilicity of a compound. In environmental chemistry, K_{ow} serves as a critical indicator for predicting a compound's bioaccumulation potential in organisms. Compounds with higher K_{ow} values tend to exhibit stronger hydrophobicity, making them more likely to accumulate in the lipid tissues of living organisms. Substances with high K_{ow} values are generally less prone to diffusion in aqueous systems and are more likely to adhere to organic matter or sediments. The K_{ow} is typically expressed on a logarithmic scale for clarity and ease of comparison. When the $\log K_{ow}$ is greater than 3, the pollutant is lipophilic and hydrophobic, so it is easier to be removed by adsorption [47,48]. Adsorption is more efficient for the removal of NCSDs with low water solubility. Some NCSDs have good biodegradability and have a good removal effect for such pollutants by biological method. The advanced oxidation method is more suitable for the removal of other refractory pollutants. In the actual WWTP and water treatment plant (WTP) water treatment process, the appropriate treatment process should also be selected according to the actual production cost.

**Fig. 1.** The route of COVID-19 drugs.

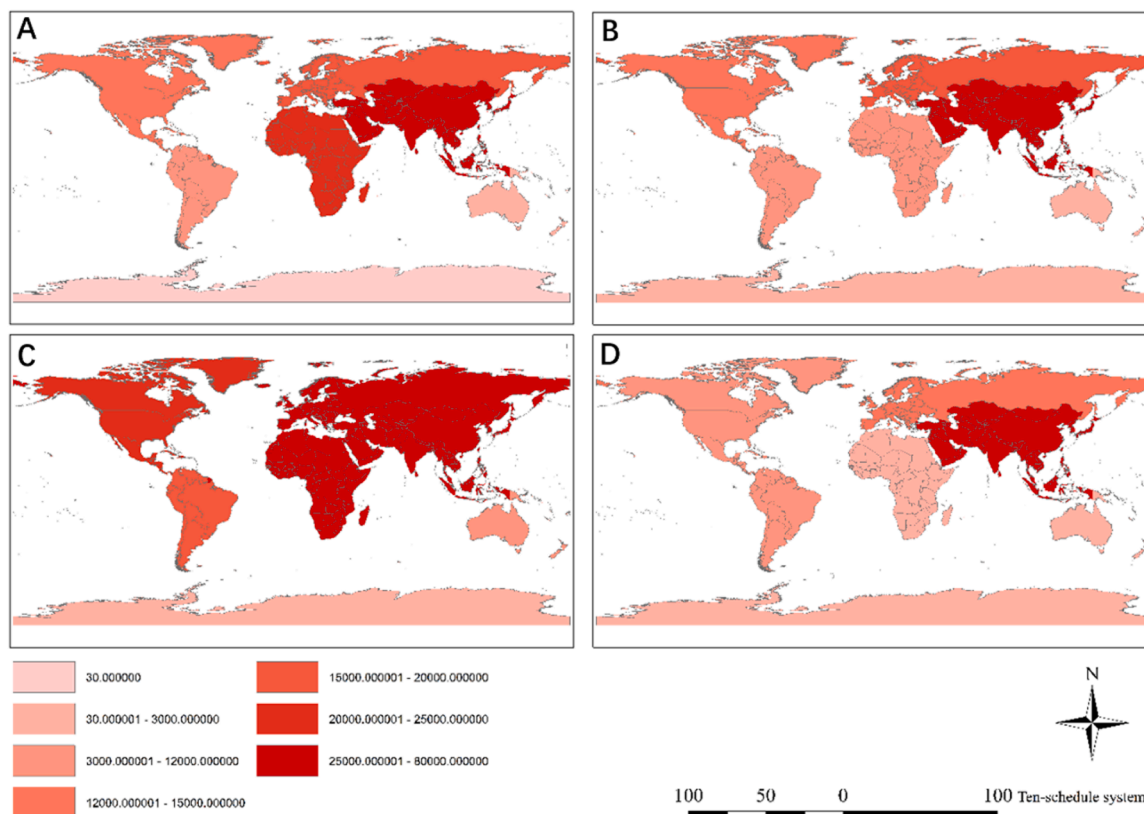


Fig. 3. Estimated global usage of COVID-19 drugs in 2023. (A) antiviral drug usage; (B) non-steroidal anti-inflammatory drug usage; (C) antibiotic drug usage; (D) immunomodulator usage. (Unit: ton) [51].

physical and chemical properties and drug detection methods.

3.1. Antiviral drugs

In the early stages of the COVID-19 outbreak, our understanding of the virus was limited. Laboratory studies identified COVID-19 as an RNA retrovirus, akin to HIV. Leveraging this characteristic, and drawing on prior experience with SARS and MERS, healthcare professionals administered a lopinavir-ritonavir combination therapy to COVID-19 patients. lopinavir-ritonavir monotherapy is recommended for first- and second-line therapy in some countries [118]. PXVD is a new oral antiviral drug [119]. PXVD consists of two components, nirmatrelvir (NAT) and ritonavir (RTV). Several previous studies showed that NAT/RTV reduced mortality rates in a 28-day follow-up by 88 % [120]. In the latest study, Sakander et al. found that molnupiravir (MPV) can be used as a viable treatment option to mitigate SARS-CoV-2 infection by reducing disease severity and mortality [121]. According to the newly released WHO treatment of novel coronavirus protocol, NAT, RDV and MPV are three antiviral drugs considered as NCSDs. NAT, RDV and MPV have played a significant role in clinical treatment. After taking the drug, the COVID-19 load in the body showed a significant downward trend, and the study confirmed that the amount of virus in the lung decreased significantly while the lung function was improved. NCSDs such as NAT, RDV and MPV will be used to fight the decline of COVID-19 for a long time in the future when humans live with COVID-19.

According to Fig. 4, it can be observed that the eight antiviral drugs ACV, Arbidol (ARB), Azvudine (AZV), CQ, MPV, RDV, RBV, and ZDV all possess hydroxyl (-OH) and amino (-NH₂) functional groups. When these functional groups are present in a chemical structure, the oxidation of -OH can lead to the formation of aldehydes or acids, thereby enhancing the water solubility of the compound. Consequently, the presence of -OH and -NH₂ functional groups increases the likelihood of these antivirals

being removed in aqueous solutions. Furthermore, ACV, Ivermectin, and OP contain ether (-O-) functional groups, which typically exhibit low photosensitivity. Thus, antiviral drugs with ether groups are not suitable for water treatment methods that rely on photocatalysis or UV irradiation. CQ's chemical structure, in addition to containing -OH and -NH₂ functional groups, features an aromatic ring, which is highly photosensitive, making UV-based removal methods more appropriate. Favipiravir (FPV) contains carboxyl (-COOH) and carbonyl (-C=O) functional groups, which enhance its polarity, and higher polarity compounds generally respond better to advanced oxidation processes. Ivermectin contains ester (-COOR) functional groups, with a macrocyclic lactone structure that is resistant to hydrolysis, although the hydroxyl and ester groups can be removed through advanced oxidation processes. LPV has an amide (-CONH₂) functional group, which increases its polarity and improves its efficiency in advanced oxidation processes. MPV, NMT, RBV, and ZDV possess carbonyl (-C=O) functional groups, and in advanced oxidation processes, reactive radicals typically attack the carbonyl group to degrade the contaminants. NVP's structure includes an azacyclic ring, which exhibits some degree of photosensitivity. RDV's structure contains a phosphate (-PO₄) group, which increases its polarity, but the phosphate group is quite stable. Therefore, to degrade RDV by attacking the phosphate group, a high oxidation potential oxidant is required. RTV contains a thioether (-S-) functional group, which can be oxidized to sulfoxide by introducing a double-bonded oxygen structure under strong oxidants, and further to sulfone, forming two double-bonded oxygen structures. This significantly increases the molecule's polarity, providing insights into the advanced oxidation degradation of RTV.

3.2. Immunomodulator

Immunomodulators are drugs or natural substances that can

Table 2
Physicochemical properties and detection methods of antiviral drugs.

Classification of Drugs	Compound name	Chemical formula	CASRN	Molecular weight (MW) (g/mol)	Solubility ^a	Detection method	pKa ^b	LogK _{ow} ^c
Antiviral Drugs	Acyclovir	C ₈ H ₁₁ N ₅ O ₃	59277–89–3	225.21	Solubility in water 0.7 mg/mL	HPLC [53]	2.27	–1.56
	Arbidol	C ₂₂ H ₂₅ BrN ₂ O ₃ S	131707–25–0	477.42	Chloroform (slightly), methanol (slightly, heated)	HPLC [54]	6.02 ± 0.50	5.40
	Azvodine	C ₉ H ₁₁ FN ₆ O ₄	1011529–10–4	286.22	Solubility in water 57 mg/mL	LC-MS [55]	9.29	–0.82
	Chloroquine	C ₁₈ H ₂₆ ClN ₃	54–05–7	319.88	Soluble in chloroform (slightly), methanol (slightly)	HPLC [56]	8.4	4.88
	Favipiravir	C ₅ H ₄ FN ₃ O ₂	259793–96–9	157.10	Soluble in DMSO (30 mg/mL), water (12 mg/mL, heated)	LC-MS/MS [57]; RP-HPLC [58]; HPLC [59]	8.77 ± 0.60	–0.58
	Ivermectin	C ₄₈ H ₇₄ O ₁₄	70288–86–7	875.11	Solubility in water 4 mg/L	HPLC [60]; LC-MS/MS [61]	12.80	3.22
	Lopinavir	C ₃₇ H ₄₈ N ₄ O ₅	192725–17–0	628.81	Solubility in DMSO 20 mg/mL	HPLC [62]; HPLC-DAD [63]	13.89 ± 0.46	4.87
	Molnupiravir*	C ₁₃ H ₁₉ N ₃ O ₇	2349386–89–4	329.31	Soluble in DMSO (slightly), methanol (slightly)	RP-HPLC [64]; LC-MS/MS [65]	2.2	–1.50
	Nevirapine	C ₁₅ H ₁₄ N ₄ O	129618–40–2	266.30	Solubility in Dimethyl sulfoxide ≥ 22 mg/mL	HPLC with UV [66]; LC-MS [67]	2.8	3.89
	Nirmatrelvir*	C ₂₃ H ₃₂ F ₃ N ₅ O ₄	2628280–40–8	499.54	Solubility in water 27.7 mg/L	HPLC [68], LC-MS [69]	10.26 ± 0.46	2.12
	Oseltamivir	C ₁₆ H ₂₈ N ₂ O ₄	196618–13–0	312.41	Soluble in methanol (slightly)	HPLC with UV [70]; LC-MS/MS [71]	7.7	0.45
	Remdesivir*	C ₂₇ H ₃₅ N ₆ O ₈ P	1809249–37–3	602.58	Solubility in ethanol is 12 mg/mL	LC/MS [72]; HPLC [73]	12.00 ± 0.70	2.40
	Ribavirin	C ₈ H ₁₂ N ₄ O ₅	36791–04–5	244.21	Solubility in water ≥ 10 g/mL	HPLC [74]; LC-MS/MS [75]	12.95 ± 0.70	–1.49
	Ritonavir	C ₃₇ H ₄₈ N ₆ O ₅ S ₂	155213–67–5	720.31	Solubility in water 5 mg/L	HPLC with UV [66]; LC-MS/MS [76]	11.47 ± 0.46	5.92
	Zidovudine	C ₁₀ H ₁₃ N ₅ O ₄	30516–87–1	267.25	Solubility in water 50 mg/mL	HPLC [77]; LC-MS [78]	9.53	0.05
Antibiotics	Amikacin	C ₂₂ H ₄₃ N ₅ O ₁₃	37517–28–5	585.61	Solubility in water 50 mg/mL	RP-HPLC [79]; LC-MS/MS [80]	8.1	–4.36
	Amoxicillin	C ₁₆ H ₁₉ N ₃ O ₅ S	26787–78–0	365.40	Solubility in water 4 mg/mL	HPLC [81]; UV-visible spectrophotometer [82]	2.4	0.87
	Azithromycin	C ₃₈ H ₇₂ N ₂ O ₁₂	83905–01–5	749.00	Insoluble in water, soluble in anhydrous ethanol and dichloromethane	HPLC with UV [83]; LC-MS/MS [84]	8.74	4.02
	Ceftazidime	C ₂₂ H ₂₂ N ₆ O ₇ S ₂	72558–82–8	546.57	Insoluble in ethanol and water	HPLC [85]; LC-MS [86]	2.77	–1.52
	Ceftriaxone	C ₁₈ H ₁₈ N ₈ O ₇ S ₃	73384–59–5	554.57	Solubility in water 40 g/mL	HPLC with UV [87]	3.2 ± 0.6	–2.64
	Ciprofloxacin	C ₁₇ H ₁₈ FN ₃ O ₃	85721–33–1	331.35	Solubility in water 86 mg/L	HPLC [88]; LC-MS [89]	4.04	0.28
	Levofloxacin	C ₁₈ H ₂₀ FN ₃ O ₄	100986–85–4	361.37	Slightly soluble in water or methanol	RP-HPLC [90]; HPLC [91]; LC-MS [91]	5.19 ± 0.40	–0.23
	Linezolid	C ₁₆ H ₂₀ FN ₃ O ₄	165800–03–3	337.35	Solubility in DMSO > 20 mg/mL	UHPLC [92]	15.53 ± 0.46	0.05
Meropenem	C ₁₇ H ₂₅ N ₃ O ₅ S	96036–03–2	383.46	Solubility in water (ultrasonic) ≥ 9.88 mg/mL	HPLC with UV [93]; LC-MS [94]	4.27 ± 0.60	–0.48	
Non-steroidal anti-inflammatory drugs	Aspirin	C ₉ H ₈ O ₄	50–78–2	180.16	Solubility in water 3.3 g/L	LC/MS-MS [95]	3.5	1.19
	Diclofenac	C ₁₄ H ₁₁ C ₁₂ NO ₂	15307–86–5	296.15	Solubility in water 1.278 mg/L	HPLC [96]; LC-MS [97]	4	4.51
	Ibuprofen	C ₁₃ H ₁₈ O ₂	15687–27–1	206.29	Insoluble in water, soluble in acetone, methanol	HPLC [98]; LC-MS/MS [99]	4.45 ± 0.04	3.97
	Indomethacin	C ₁₉ H ₁₆ ClNO ₄	53–86–1	357.79	Solubility in acetone, ethanol (20 mg/mL) insoluble in water	HPLC [100]; LC-ESI-MS-MS [101]	4.5	3.68
	Ketoprofen	C ₁₆ H ₁₄ O ₃	22071–15–4	254.29	Solubility in water 209 mg/L	HPLC with UV [102]; LC-MS [103]; LC-MS/MS [104]	5.94	3.12
	Naproxen	C ₁₄ H ₁₄ O ₃	22204–53–1	230.26	Insoluble in water, soluble in ethanol and methanol	HPLC [105]; LC-MS/MS [106]	4.28 ± 0.02	3.18

(continued on next page)

Table 2 (continued)

Classification of Drugs	Compound name	Chemical formula	CASRN	Molecular weight (MW) (g/mol)	Solubility ^a	Detection method	pKa ^b	LogK _{ow} ^c
	Paracetamol	C ₈ H ₉ NO ₂	103-90-2	151.17	Solubility in water 14 g/L	HPLC [107]; LC-MS [108]	9.86 ± 0.13	0.46
Immunomodulator	Baricitinib [*]	C ₁₆ H ₁₇ N ₇ O ₂ S	1187594-09-7	371.12	Solubility in DMSO 30 mg/mL	RP-HPLC [109]; LC-MS [110]	11.66 ± 0.50	1.08
	Dexamethasone	C ₂₂ H ₂₉ FO ₅	50-02-2	392.47	Solubility in water 10 mg/100 mL	HPLC [111]; LC-MS [112]	12.13 ± 0.70	1.83
	Leflunomide	C ₁₂ H ₉ F ₃ N ₂ O ₂	75706-12-6	270.21	Insoluble in water, soluble in methanol	HPLC [113]	10.8	2.36
	Methylprednisolone	C ₂₂ H ₃₀ O ₅	83-43-2	374.48	Solubility in water 0.12 g/L	LC-MS/MS [114]	12.46 ± 0.70	1.60

Notes: CASRN (Chemical Abstracts Service Registry Number); LogK_{ow} (Logarithm of the octanol-water partition coefficient); HPLC (High-Performance Liquid Chromatography); RP-HPLC (Reversed-Phase High-Performance Liquid Chromatography); HPLC-DAD (High-Performance Liquid Chromatography with Diode Array Detector); LC-MS (Liquid Chromatography-Mass Spectrometry); HPLC with UV (High-Performance Liquid Chromatography with Ultraviolet Detection); UHPLC (Ultra-High Performance Liquid Chromatography); MS (Mass Spectrometry); LC-ESI-MS-MS (Liquid Chromatography-Electrospray Ionization Tandem Mass Spectrometry).

^{*} WHO recommended medication for 2024

Source: ^a ^c from [115], ^b from [116], ^d from [117].

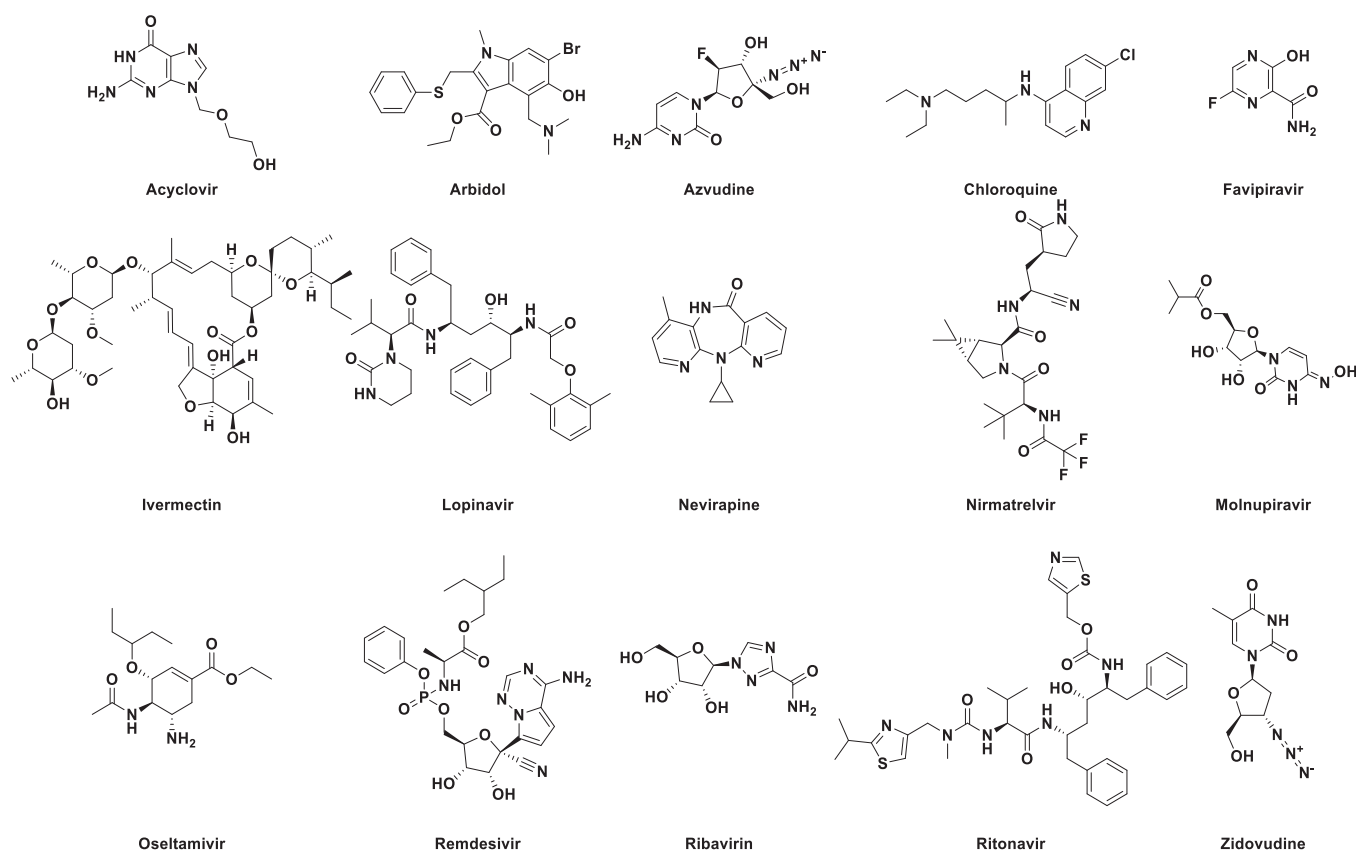


Fig. 4. The chemical structure of the antiviral drug used in the COVID-19 epidemic [115].

influence the function of the immune system, primarily encompassing immune enhancers and immunosuppressants. As drug development continues to progress, treatment of hospitalized patients with COVID-19 has shifted from untargeted treatment to mildly effective antiviral drugs, to immunomodulatory therapies that reduce mortality [122]. Some studies have shown improved outcomes in patients with progressive and critically ill COVID-19 who received either tocilizumab or salizumab combined with corticosteroids [123]. Bekta et al. injected two kinds of glucocorticoids, anakinra (ANK) and baricitinib (BCB), into critically ill patients with COVID-19. Clinical results showed that the mortality rate and tracheal intubation rate of patients after intravenous ANK and BCB treatment were 46.7%. Compared with the control group, the mortality

rate and tracheal intubation rate were decreased by 69.8% [124]. Liu et al. found that a single dose of pulse methylprednisolone (40–500 mg) had no significant negative effects on SARS-CoV-2 removal and specific IgG production, while effectively blocking the inflammatory cascade [125]. Clinically, the use of immunomodulators provides a new idea for the clinical treatment of COVID-19 in the future, not only reducing the number of COVID-19 carriers, but also regulating the immune system in patients to enhance immune capacity and avoid other side effects.

As shown in Fig. 5 BCB contains -NH₂, -S=O, -CN, and a pyridine ring. The -NH₂ and -S=O groups are susceptible to attack by reactive radicals, while the -CN and pyridine ring structures exhibit higher stability. Therefore, it is recommended to use strong oxidizing agents when

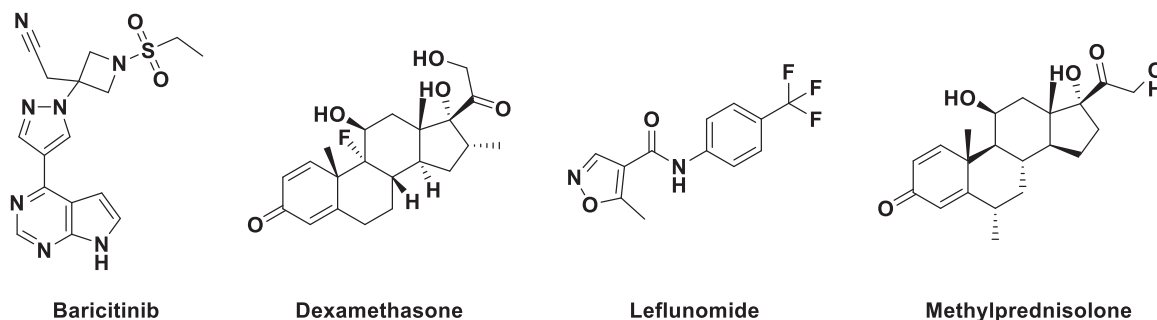


Fig. 5. The chemical structure of the immunomodulator drug used in the COVID-19 epidemic [115].

reacting with BCB. DEX contains a C=C bond, which typically has lower stability. During the oxidation process, oxidizing agents may initially target and cleave the C=C bond. Leflunomide's structure includes an isoxazole ring, a formamide group (-NH-CO-), and an aromatic ring. The -NH-CO- group can degrade through hydrolysis, while the benzene ring structure provides some stability, making it removable under strong oxidative conditions. Methylprednisolone contains a cyclohexane ring, a cyclopentane ring, and two C=C bonds, imparting a certain level of stability to the molecule. During oxidation, the oxidizing agents are likely to first attack and break the C=C double bonds, followed by subsequent attacks on the cyclohexane and cyclopentane ring structures.

3.3. Non-steroidal anti-inflammatory drugs

Combined with clinical feedback from laboratories and hospitals, the main clinical symptoms of COVID-19 are fever, dyspnea, sore throat, weakness of limbs, dizziness, and nausea [126]. Qiao et al. reported that 70 % of patients' body temperature fluctuated in the range of 36.5°C to 38.8°C [127]. Before the advent of NCSDs, symptomatic treatment strategies were used for people infected with COVID-19. Traditional antipyretic and analgesic drugs include ibuprofen (IBU), acetaminophen (APAP), aspirin (ASA) and etc. Clinical trials confirm the safety of APAP and IBU in patients with COVID-19 [128]. The use of such drugs has risen sharply during the outbreak. In late December 2022, the highest concentration of ASA detected by WWTP in urban China reached 10,000 mg/d/inch, the highest concentration of ASA detected by WWTP in rural China reached nearly 900,000 mg/d/inch, and the highest concentration of ibuprofen reached nearly 10,000 mg/d/inch [129]. This may be because antipyretic and analgesic drugs such as IBU and ASA are inexpensive and available over the counter, making them more accessible to residents and ultimately leading to a significant increase in use. As routine clinical treatment drugs, IBU, APAP and ASA are widely used worldwide in the environmental matrix, and the concentration changes

and toxicity risks of non-steroidal anti-inflammatory drugs are worthy of attention, and relevant studies are worthy of environmental risk assessment in the future.

Non-steroidal anti-inflammatory drugs have relatively simple structures, as illustrated in Fig. 6 They all feature a benzene ring, which contributes to their stability. Additionally, these drugs contain amide (-CONH-) and indole ring structures. The -CONH- group can be hydrolyzed, while the indole ring is highly stable. Naproxen (NPX) contains a methoxy (-OCH₃) group, which is readily oxidized during the oxidation process, leading to the formation of more polar substances.

3.4. Antibiotics

Antibiotics are used to treat bacterial infections. In the treatment of COVID-19, antibiotics are not used to fight COVID-19 itself, but to prevent bacterial infections caused by COVID-19, such as bacterial pneumonia, sepsis and other complications. In the early days of the COVID-19 outbreak in Wuhan, antibiotic treatment was used as one of the treatments [130]. In one Scottish hospital, AMX accounted for 22 % of the prescriptions given to COVID-19 patients, doxycycline (DOX) accounted for 17 % and ciprofloxacin (CIP) accounted for 3.2 % [131]. In the treatment of severe patients, the combination of antiviral drugs and amoxicillin accounted for about 60 %, followed by the combination of antiviral drugs and cephalosporin (CEP) accounted for about 16 %. Although studies have shown that antibiotic treatment does not improve the clinical symptoms of COVID-19 patients, more than 80 % of hospitalized patients are still receiving antibiotics because almost all infected patients have weakened immunity, which increases the risk of bacterial infection. AMX, CEP, DOX, CIP and other drugs used in large quantities in the COVID-19 epidemic are bound to cause concentration changes in the environment, increasing environmental risks. The traditional treatment process of WWTP has limited degradation efficiency for antibiotics, and even high antibiotic concentration can lead to decreased

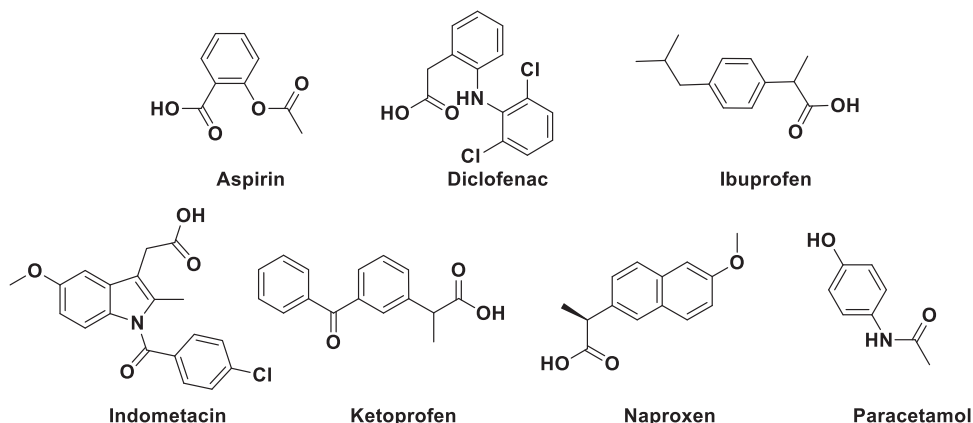


Fig. 6. The chemical structure of the non-steroidal anti-inflammatory drug used in the COVID-19 epidemic [115].

treatment efficiency. In WTP, the removal efficiency of the coagulation precipitation process is about $11.3\% \pm 26.4\%$, that of sand carbon filtration is about $1.7\% \pm 21.4\%$, and that of chlorine disinfection is about $48.7\% \pm 11.9\%$, and there are great differences in the removal efficiency of different types of antibiotics. The stability of antibiotic removal efficiency cannot be guaranteed [132].

As shown in Fig. 7, amikacin with its multiple aminoglycoside groups, is relatively stable in acidic environments. Consequently, neutral or alkaline conditions may be more effective for its degradation. AMX, ceftazidime, and ceftriaxone each feature a β -lactam ring, which is prone to hydrolysis. Azithromycin contains a macrolide ring structure, which enhances its stability, but it also shows some photosensitivity, suggesting that photocatalysis or UV methods might be effective for its removal. CIP and levofloxacin have fluoroquinolone structures that increase their stability. Linezolid features an oxazolidinone structure, which provides good stability. Due to its polarity and ring structure, oxazolidinone may interact with certain enzymes in biodegradation processes, potentially enhancing the effectiveness of biological methods for removing linezolid. Meropenem contains a carbapenem structure, which is susceptible to hydrolysis. The carbapenem structure includes a

five-membered ring connected to a β -lactam ring with various side chains, which increases its chemical stability.

4. Removal methods of COVID-19 drugs

4.1. Biological method

Biological water treatment technology leverages the metabolic capabilities of microorganisms to convert organic substances and pollutants in water into simpler, harmless compounds. This approach offers significant environmental benefits as it avoids the need for large quantities of chemical agents and reduces the generation of chemical waste. Compared to traditional physicochemical treatment methods, biological treatment is typically more cost-effective, particularly for long-term operations, with lower operation and maintenance costs. Renowned for its high efficiency and sustainability, biological treatment technology is a key option in modern water treatment practices. As shown in Table 3, this study reviews the efficiency and conditions of biological removal of COVID-19 drugs in water.

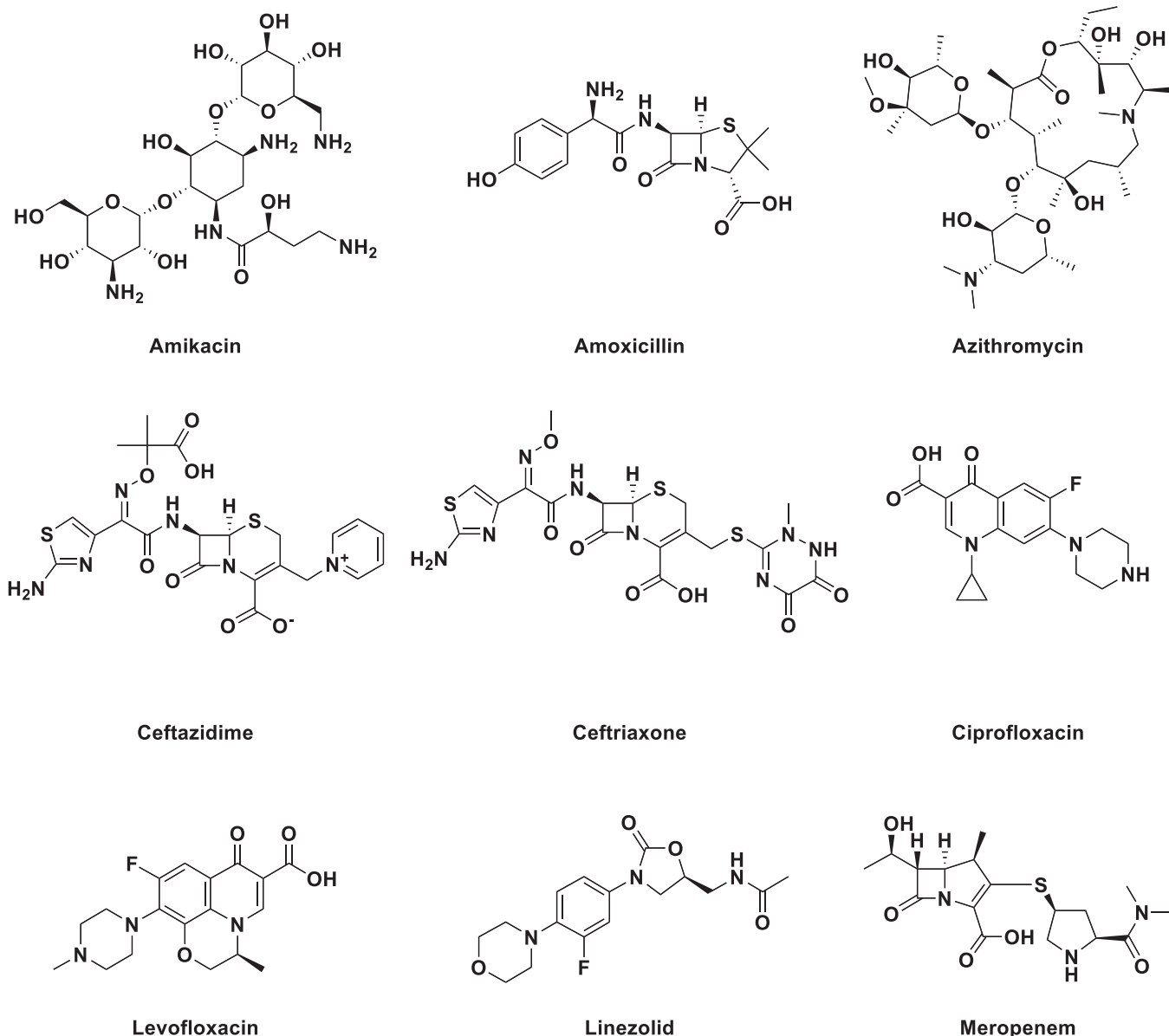


Fig. 7. The chemical structure of the antibiotic drug used in the COVID-19 epidemic [115].

Table 3
Biological removal methods for COVID-19 drugs.

Drugs	Concentration	Removal Technique	Removal rate	References
Acyclovir	170 mg/L	Activated sludge process	> 90 %	[133]
	600 ng/L	Aerobic treatment system	80 %	[134]
	154 mg/L	Membrane bioreactor	98 %	[135]
Arbidol	0.5–10.0 mg/L	Removal of ARB by <i>M. aeruginosa</i>	49.8 %–72.4 %	[136]
Azvadine	/			
Chloroquine	51.6 mg/L	Membrane bioreactor	98.2 %	[137]
Favipiravir	8 mg/L	Activated sludge process	35 %	[138]
Ivermectin	800 ng/L	Activated sludge process	100 %	[139]
	709 ± 544 ng/L	Artificial wetlands	97 %	[140]
	0.1 µg/L	Granular activated carbon biological filter + ultrafiltration	63 %	[141]
Lopinavir	21–829 ng/L	A ² /O treatment process	96 %–98 %	[3]
	21–829 ng/L	CASS treatment process	–50 %	[3]
Molnupiravir	/			
Nevirapine	0.41–1.59 ng/L	A ² /O/MBR treatment process	48 %	[3]
Nirmatrelvir	/			
Oseltamivir	10 mg/L	Microalgal bioremediation	100 %	[142]
	20 mg/L		63 %	
	30 mg/L	54 %		
	5–100 ng/L	Activated sludge process	< 50 %	[143]
Remdesivir	10 mg/L	Novel, continuous-flow, helical-baffle incorporating VUV/UVC photoreactor	67.9 % (10 min)	[144]
		Moving bed bioreactor (MBBR)	31.1 %	[145]
Ribavirin	1 mg/L	Bio-Electro-Fenton (BEF) system	70.2 %	[146]
	2 mg/L			
Ritonavir	110 ng/L	A ² /O treatment process	97 %–99 %	[3]
	110 ng/L	CASS treatment process	25 %–65 %	[3]
Zidovudine	3596 ng/L	Trickling filter + Stabilization ponds	88.4 %	[147]
	4202 ng/L	Decentralized Treatment Facility	70.5 %	[147]

The removal conditions are shown in Table S1.

/: Not found in existing studies.

4.1.1. Activated sludge method

The activated sludge method has the advantages of strong adaptability, stable system and low operating cost, and activated sludge can be recycled and reused, which meets the requirements of environmentally sustainable development.

Victoria Osorio et al. investigated the removal mechanism of DCF and anti-inflammatory drugs with similar structures in nitrification sludge reactors. During the nitrification reaction, NO[·] will be produced, which is a highly active substance. Under anaerobic conditions, molecular oxygen and NO[·] will generate nitrous oxide (N₂O₃). The presence of superoxide radical anion (O₂^{·-}) in the system produces peroxyntirite (ONOO⁻), ONOO⁻ and N₂O₃ have higher activity than NO[·] [148]. It has been reported that there are differences in the degradation efficiency of nitrifying activated sludge for different types of anti-inflammatory drugs, which is due to the presence of certain functional groups,

forming steric hindrance [149]. The poor effect of drug degradation also depends on the presence of halogens and aromatic amines in their chemical structure. However, the microorganisms present in the nitrifying microbial community in activated sludge can be used to degrade the pollutants [150]. Park proposed the degradation of APAP by microbial communities in activated sludge. After one month of acclimation with APAP, the degradation rate of the activated sludge reached 95 %, which was 8 times higher than that of the initial unacclimated activated sludge. Park isolates the *Pseudomonas* species group (PCO) from the APAP degradation community. The efficiency of APAP removal in the activated sludge inoculated with PCO reached 590 mg/L, and APAP would eventually decompose into APAP-derived metabolites, 4-aminophenol, hydroquinone and 1, 4-benzenone [151]. DEX as a hormone drug, the concentration reached the level of µg/L. Liu et al. investigated the effect of DEX on SBR reactors. It was found that when the DEX concentration was increased to 500 and 1000 µg/L, the removal efficiency decreased to 72.4 % and 30.8 %, respectively. This may be because DEX inhibits the ability of activated sludge to remove C and N. During the first 15 days after adding DEX, effluent chemical oxygen demand (COD) and total nitrogen (TN) both fluctuate to some extent, but long-term studies show that effluent quality is relatively stable. This may be due to the gradual increase in the ammoniacal oxidation activity of activated sludge in the long-term presence of DEX, while the ammoniacal oxidation activity has not reached the level of treated DEX in the initial stage, resulting in the fluctuation of TN [152]. Xu et al. found that free nitrite (FNA) is an important factor in inhibiting ammonia-oxidizing bacteria (AOB) ammonia oxidation and FPV degradation. When the concentration of FNA was 0.07 and 0.02 mg-N/L, the removal efficiency of FPV reached 12.6 % and 35.0 %, respectively. Although FNA inhibits the cell's production of ATP [152]. As a result, the energy of the microbial community in the activated sludge is insufficient, resulting in decreased activity, but at a lower concentration, it can still work with AOB ammonia oxidation to remove FPV [138].

4.1.2. Membrane bioreactor (MBR)

MBR as a relatively mature water treatment process, MBR has many advantages, including high permeability, low sludge yield, high mixed liquid suspended solids concentration, low environmental impact, and small footprint. Therefore, MBR systems are widely used in wastewater treatment, especially when high water discharge is required and space is limited [153], WWTP and WTP have great potential for removing new pollutants such as NCSDs.

Gonzalez-Perez studied the degradation effects of nonsteroidal anti-inflammatory drugs IBU, DCF, ketoprofen (KPF) and NPX in biofilm reactors [154]. The removal rate of IBU, NPX and KPF reached more than 95 %, but the removal efficiency of DCF was very low, and the highest removal rate reported in the literature was only 53.4 % [155]. It is reported that prolonged hydraulic retention time (HRT) is of great help to the removal of pollutants, because by extending HRT, the pollutants are in contact with and fully react with the biofilm components, in which the biodegradable part reaches 100 %. DCF is hydrophilic and has low biodegradability [156]. Obviously DCF is not suitable for biological removal. Gutierrez studied the effect of powdered activated carbon (PAC) on the degradation efficiency of MBR [157], and found that the degradation efficiency of DCF, caffeine, ofloxacin, SMX and amphetamine was significantly improved after PAC was added. This may be attributed to the adsorption of contaminants by the PAC, which in turn improves the contact time with the MBR, allowing it to fully react. Liu et al. evaluated the effect of anaerobic biofilm reactors on the removal of fluoroquinolones, sulfonamides, and tetracycline antibiotics. The results showed that the removal rate of tetracycline drugs could reach 100 %, while the removal efficiency of fluoroquinolones and sulfonamides was lower, which were 35–64 % and 21–71 %, respectively [158], and showed poor biodegradability [159,160]. The removal rate of tetracycline drugs is high. We analyzed from the perspective of chemical structure, which may be due to the presence of amides and

carboxyl groups in the structure of tetracycline drugs, and the biofilm adsorbs them by electrostatic attraction [161], which improves the biodegradation effect. In contrast, complex heterocyclic substituents in sulfonamides, such as pyrimidine in sulfadimethazine and pyridine in sulfadiazine, significantly impede their biodegradation. These heterocyclic substituents induce strong spatial blocking effects by increasing molecular volume and structural complexity, making it difficult for microorganisms or enzymes to effectively degrade these compounds [162]. Arriaga et al. used MBR process to remove ACV, and its maximum degradation rate reached about 90 % [163]. When the target pollutant has good hydrophobicity, or some groups with poor biodegradability such as $-\text{CONH}_2$, $-\text{CONHR}$ and $-\text{CONR}_2$ [164], MBR process or other biological methods usually cannot achieve better removal effect. For example, carbamazepine (CBZ) removal rates were reported to be only 0.3–39.2 % [164], and 1.0–28.3 % for IBU [165].

4.1.3. Microbial fuel cell (MFC)

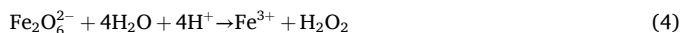
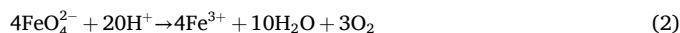
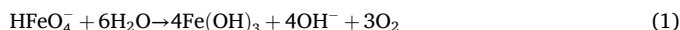
A microbial fuel cell is a system that converts chemical energy generated by the metabolic activities of organisms into electrical energy. Often anaerobic microorganisms in the anode chamber of MFC perform metabolic activities using pollutants as carbon sources. Protons and electrons are produced as anaerobic microbes degrade pollutants [166], and the oxidation reduction reaction occurs in the cathode chamber to achieve the removal of pollutants. MFC combines the characteristics of biological method and electrochemical method, reduces the production cost, and the by-products generated by the reaction are mainly H_2O and CO_2 , which has the advantages of environmental friendliness. Utami et al. explored the degradation of paracetamol by microbial batteries and found that *Burkholderia* dominated the microbial community in MFC by analyzing the types and quantities of microbial communities in MFC [167]. *Burkholderia* not only has the ability of electron transfer, but also can degrade large molecules into simple small molecules, and the degradation rate of paracetamol reached 48.69 ± 0.86 % when the pH value was 8.2. It has been reported that MFC has an excellent degradation effect on antibiotics, the degradation rate of penicillin in MFC is 98 %, the degradation rate of SMX is 87.52 ± 1.97 % [168], and the degradation rate of oxytetrin is 99 % [169]. At present, the published literature focuses on the degradation of MFC to antibiotics and non-steroidal anti-inflammatory drugs, while there are still a lot of gaps in the research of MFC on NCSDs such as antiviral drugs and immunomodulators in the COVID-19 epidemic. The degradation of new pollutants such as NCSD by MFC is one of the future research directions.

4.2. Non-biological method

4.2.1. Advanced oxidation method

Advanced oxidation process (AOP) is a treatment approach that degrades pollutants by generating highly reactive oxygen species (ROS). the advanced oxidation method is not only capable of generating strongly oxidizing active free radicals within a short period. Simultaneously, the end product of the advanced oxidation process is mainly H_2O and CO_2 , which constitutes a green and environmental friendly water treatment procedure. As shown in Fig. 8 and Table 4, this study reviews the application of advanced oxidation processes, including ferrate, ozonation, ultraviolet, electrochemical oxidation, permanganate, and photocatalysis, in the treatment of COVID-19 pharmaceuticals.

4.2.1.1. Ferrate(VI). Ferrate is a new kind of water treatment agent. Although ferrate is not commonly employed in conventional water treatment processes, its application in the pre-treatment stage has demonstrated significant effectiveness, particularly during major public health emergencies. Fe(VI) is a strong oxidizing agent with a reduction potential of 2.20 eV [200]. In the process of degradation of pollutants, Fe(VI) will undergo a redox reaction with the target pollutants, and first decompose into Fe(V) and Fe(IV) with high activity. Fe(V) and Fe(IV) will further degrade the pollutants, among which Fe(IV) will self-decompose and produce H_2O_2 , which helps to improve the removal efficiency of pollutants. Fe(VI) eventually breaks down into Fe(III) and Fe(II) . The main reaction formula is shown in formulas (1)–(8), and the Fe(III) generated at the same time has the effect of adsorption coagulation to further remove the residual pollutants [201,202].



Suyamud et al. investigated the removal of AMX, oxytetracycline

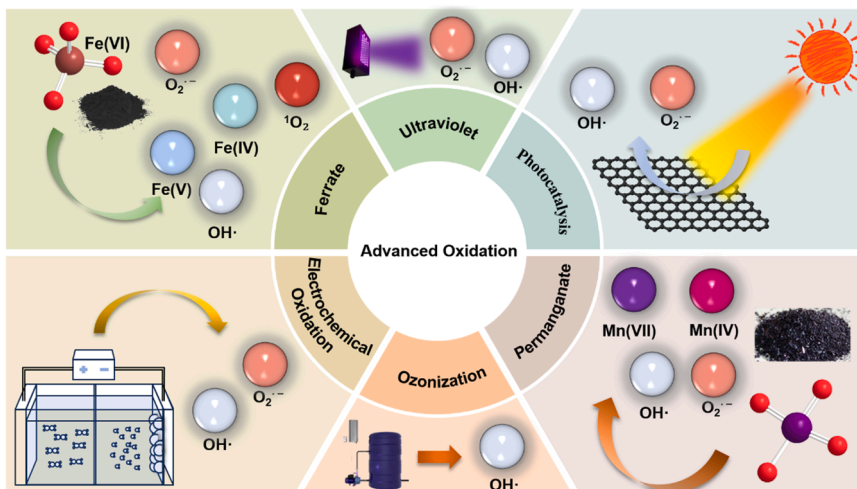


Fig. 8. Schematic diagram of advanced oxidation method.

Table 4
Non-biological removal methods for COVID-19 drugs.

Drugs	Concentration	Removal Technique	Removal rate	References
Acyclovir	10 mg/L	Photo-Bio-Electro-Fenton (PBEF)	100 %	[170]
	100 μM	Photocatalysis	100 %	[171]
	400 mg/L	Adsorption	90.3 %	[172]
Arbidol	40 μM	Phosphate/peroxymonosulfate	100 %	[173]
	20 mg/L	Electrochemical oxidation	96–98 %	[174]
	20 mg/L	MOFs material adsorption	100 %	[175]
Azvadine	/			
Chloroquine	125 mg/L	Electrochemical oxidation	100 %	[176]
	6 mM	UV/H ₂ O ₂ process	73.7 % (10 min)	[177]
	10 μM	Ferrate	100 % (20 min)	[178]
	100 mg/L	Adsorption	90.37 % (25 min)	[179]
Favipiravir	0.4 mM	Electrochemical oxidation	89.5 % (20 min)	[180]
	100 μg/L	Photocatalysis	99 % (7 h)	[57]
Ivermectin	80 mg/L	Electrochemical oxidation	100 % (saturating O ₂ and passing current)	[181]
	0.5 mg/L	UV / TiO ₂ process	98 % (10 min)	[57]
	500 μg/L	Adsorption	≥ 96 %	[182]
Lopinavir	100 μg/L	Ferrate	25 %	[183]
	200 mg/L	Adsorption	78 % (after five cycles)	[184]
	10 mg/L	Photocatalysis	95 % (60 min)	[185]
Molnupiravir	32.93 mg/L	Electrochemical oxidation	100 %	[186]
Nevirapine	10 mg/L	Photocatalysis	100 %	[187]
	5–20 ppm	Photocatalysis	68 %	[188]
	1 mg/L	Adsorption	95–99 %	[189]
Nirmatrelvir	/			
Oseltamivir	1 μM	Ozonation	> 50 %	[190]
Remdesivir	1 mg/L	Photo-electrocatalytic process	92 % (2 h)	[191]
	125 mg/L	Adsorption	93 %	[192]
	10 mg/L	Photolysis	98 %	[193]
	10 mg/L	Photocatalysis	91.6 % (30 min)	[194]
	10 μM	Ozonation	50 % (5 min)	[195]
Ribavirin	41.5 μM	Ferrate	91.68 % (120 min)	[196]
	1 μM	UV/H ₂ O ₂ process	71 %	[197]
	1 μM	UV/PDS process	90 % (60 min)	[197]
	10 mg/L	Photocatalysis	95 % (15 min)	[185]
Ritonavir	0.5 mg/L	Adsorption	75.1 ± 0.9–92.8 ± 0.1 %	[198]
	1 g/L	Ozonation	/	[78]
Zidovudine	10 mg/L	Sono-electrochemical degradation	69.09 %	[199]

The removal conditions are shown in Table S2.

/: Not found in existing studies.

(OTC) and enrofloxacin (ENR) by Fe(VI) in deionized water and shrimp aquaculture water, and the removal rate of OTC is close to 100 % [203]. This may be due to the presence of electron-rich phenolic groups in the chemical structure of OTC, with which ferrates react to degrade. However, olefin and amine groups are the main chemical structures of AMX and ENR [204], additionally, the study revealed that Fe(VI)'s reactivity with olefin and amine groups is lower compared to its reactivity with electron-rich classification groups, so the degradation efficiency is slightly worse. The highest removal efficiency of ENR reaches 84 %, and the highest removal efficiency of AMX is close to 60 %. Wang et al. studied the process of ferrate degradation of APAP and showed that the removal efficiency of APAP can be as high as 99.6 % within 5 min [205]. The study also found that ferrate exhibits high degradation efficiency for highly protonated APAP, which is because the chemical structure of APAP has a phenol structure. Based on this discovery, ferrate may also have a high degradation effect on compounds with phenol chemical structure in COVID-19 drugs. Li et al. investigated the removal of the antiviral drug RBV by ferrate. It was found that when the molar ratio [Fe(VI)]:[RBV]= 60:1, the removal efficiency of RBV was about 91.68 % within 120 min, and when [Fe(VI)]:[RBV]= 30:1, the removal efficiency was 81.70 % [206]. Although the concentration of Fe(VI) is doubled, the removal efficiency is not significantly improved, which may be because Fe(VI) itself has a high redox potential of 2.20 V, resulting in Fe(VI) has a strong ability to seize electrons, so that Fe(VI) has a self-decay phenomenon within a certain period of time, resulting in its oxidation capacity weakened. The quenching test showed that the main active substances for RBV degradation in Fe(VI) system were •OH

(12.91 %), Fe(V)/Fe(IV) (13.83 %), Fe(VI) (73.26 %). It has been established that Fe(VI) plays a primary role in the degradation of RBV. As shown in Fig. 9, Fe(VI) initially attacks the amide group of the RBV molecule, leading to the destruction of the amide group and the formation of a carboxyl group, resulting in the intermediate P1. Subsequently, the carboxyl group of P1 is substituted by hydroxyl and hydrogen atoms, forming intermediates P2–1 and P2–2. Next, the carbon-nitrogen bond in the triazole ring of P2–1 breaks, while P2–2 reacts at the hydroxymethyl group connected to the ribose. Through these degradation pathways, RBV is ultimately broken down into non-toxic, harmless substances. Li et al. also used ferrate/acetylpyruvate (AA) system to degrade RBV, and degraded RBV by producing Fe(IV), Fe(V), •OH, CH₃ and -CHO active free radicals. The concentration ratio [Fe(VI)]:[AA] = 4:1, the degradation efficiency reached 73.70 % in 15 min, which was significantly higher than that of 51.38 % for RBV degradation by ferrate alone [207]. The results show that organic free radicals play a major role in the system. At present, the degradation of new pollutants by ferrate is mainly concentrated in antibiotics, and there are few studies on the degradation of antiviral drugs by ferrate, especially the degradation of antiviral drugs by ferrate combined system is worthy of further study.

4.2.1.2. Ozonation. Ozonation is a kind of advanced treatment technology in water treatment technology, usually when the water quality of the conventional treatment process does not meet the requirements of the standard specification, additional treatment technology. Ozone and hydroxyl radicals attack the electron-rich part of the target pollutant,

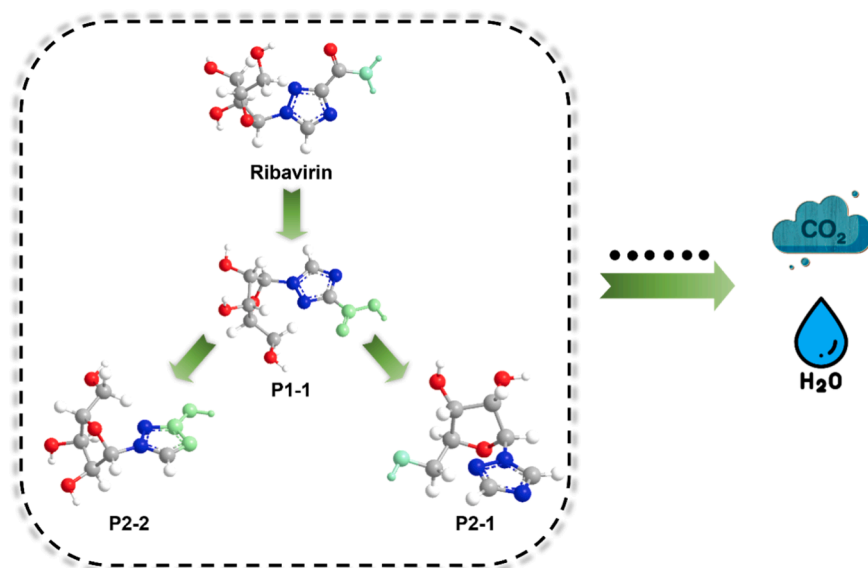
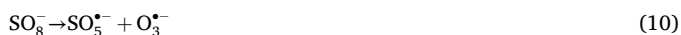


Fig. 9. Mechanism of RBV degradation by ferrate [206].

achieving the effect of degrading the pollutant.

Jing et al. compared the removal effects of UV/O₃, UV alone, and O₃ alone on the degradation of ibuprofen (IBU) in water. The study found that a 0.6 mol/L UV/O₃ system achieved a 100 % degradation rate within 20 min, while a 0.6 mol/L O₃ system alone reached only 82 % degradation after 80 min. Quenching tests indicated that ozone molecules played a dominant role in IBU degradation. However, the addition of tert-butanol (TBA) resulted in a 90 % removal rate, highlighting the significant role of UV in the system. The degradation process produced 11 transformation products with -OH and -COOH groups, which was fewer than the 17 transformation products generated by O₃ alone [208], and UV/O₃ TPs has lower ecotoxicity and lower economic cost in production investment. Funke studied the process of ozone degradation of ZDV and found that ZDV can be completely removed when the ratio of O₃ to ZDV is 2:1. The study also analyzed the TPs of ZDV. O₃ first attacked the C-C double bond in the chemical structure of ZDV, causing it to decompose into nine equivalent TPs. In the degradation process, O₃ did not attack the nucleoside part of ZDV, but concentrated on the nuclear base [78]. The azide part of ZDV remains stable, and the azide part is not attacked by active free radicals during the degradation of O₃. Liu et al. studied the removal process of the antiviral drug RBV in O₃/peroxymonosulfate (PMS) system. This system mainly produces •OH and SO₄^{•-} two kinds of reactive free radicals, which mainly act on •OH. The formula of free radical formation is shown in (9)–(12). The reaction rate constants between RBV and •OH and SO₄^{•-} are 1.9 × 10⁹ M⁻¹ s⁻¹ and 7.9 × 10⁷ M⁻¹ s⁻¹, respectively. RBV is first dehydrogenated at the hydroxyl group and then loses the amide or methanol group. The removal rate of RBV in O₃/PMS system exceeds 50 % within 2 min, while the removal rate of RBV in O₃ degradation alone is only about 20 % within 2 min.



4.2.1.3. Ultraviolet. Huang et al. studied the degradation mechanism of RDV, HCQ and DEX in the combined UV and H₂O₂ system [193]. It is reported that RDV, HCQ and DEX can be completely degraded by up to 160 s. Among them, the mineralization rate of RDV is only 14 %, which

is much different from HCQ (50 %) and DEX (44.5 %). As a nucleoside antiviral drug, RDV has nucleotide groups in its structure [209]. This is different from DEX and HCQ, through the comparison of RDV and DEX, HCQ chemical structure formula found that RDV also has a complete benzene ring structure, which is speculated to be one of the reasons for the low mineralization rate, the subsequent density functional theory (DFT) simulation calculation also confirmed this point. The degradation of RDV is caused by •OH attacking the C atom with the largest atomic potential, resulting in the break of chemical bonds, and the chemical bonds of the generated TPs are not stable enough, and the •OH in the system is easy to crack it, thus achieving removal. The removal mechanism of DEX as an immunomodulator is slightly different, mainly through the substitution of hydroxyl by aromatic ring, the substitution of C-F bond by -OH, and the attack of •OH on dihydroxyacetone and C. The final degradation efficiency is DEX > HCQ > RDV. The effective destruction of nucleotide groups in the chemical structure of nucleoside antiviral drugs such as RDV is worthy of further study. Wu et al. studied the mechanism of RBV removal by UV/TiO₂/H₂O₂ system, and the research showed that the removal efficiency of RBV reached 97.8 % and the mineralization rate was 53.3 % within 20 min, which did not achieve the effect of complete mineralization. In the actual medical wastewater, the RBV removal efficiency of the UV/TiO₂/H₂O₂ system reached 80 %, which only reflects the advantages of the UV/TiO₂/H₂O₂ system for RBV degradation. The system mainly produces •OH and O₂⁻ active free radicals. Although the toxicity risk of the final degradation product is low, in the initial TPs, due to the incomplete mineralization of RBV, toxicity increases compared to the toxicity of RBV itself. Given the current low mineralization rate of antiviral drugs by oxidation technology, future studies can explore how to improve the mineralization rate of antiviral drugs. It can also focus on different UV co-use systems, and the combined effect of multiple oxidation technologies is better than that of a single system to degrade drugs.

4.2.1.4. Electrochemical oxidation. Electrochemical oxidation is an advanced oxidation technology, which has the advantages of simple operation and controllable cost. Zhang et al. for the first time used carbon Fe₃O₄-doped montmorillonite (Mt) particle electrodes to degrade ARB and ACV in the electro-fenton system [174]. Mt./GH/Fe₃O₄ electrodes were prepared with FeCl₃, NaAc and PEG by using Mt as a carrier and sucrose as carbon source. The study shows that the removal rate of ARB and ACV in the system is also higher when the applied voltage is higher, and the removal rate of ARB and ACV is close

to 100 % after 15 min of reaction. It was also found that the removal rate of ACV can be increased from 45 % to 91 % under aeration conditions, but the increase in pollutant removal rate is not obvious when the aeration concentration is too high, which may be related to the reduction of the contact area between the catalytic electrode and pollutants [210]. Zhou et al. prepared porous Ti/SnO₂-Sb anode antiviral drug ABC with permeable flux and conducted degradation tests. The results show that the degradation efficiency of ABC can reach 97 % when the current density is 0.2 mA cm⁻² for 10 min [211]. The degradation process mainly attacks the ABC cyclopropyl structure and the cyclopropylamine structure, in which the cyclopropylamine structure generates acetamide structure after losing C and N atoms, thus achieving the purpose of degradation. The minimum energy consumption is only 6.5 m WhL⁻¹, and the ecological environmental toxicity is also greatly reduced. In the current study, titanium coated electrode, glass carbon electrode, graphite electrode, platinum electrode, titanium platinum electrode, doped diamond electrode and other different composite materials are used to prepare electrodes, but there are few studies on bio-based electrode materials, such as sucrose derivatives and other environmentally friendly bio-based materials. The combination system of electrochemical technology and other advanced oxidation technology is also the future research and development direction. At the same time, in the study of electrochemistry in water treatment, the selection of pollutants is still concentrated on antibiotics or traditional antiviral drugs, such as ACV, ABC, etc. The research on FPV, NAT and other NCSDs is still in its infancy, and NCSDs can be selected as the target pollutants for future research.

4.2.1.5. Permanganate. Permanganate is a strong oxidizing agent [212], commonly used in water treatment, MnO₂, one of the products of permanganate, has flocculation in the water treatment process, removing contaminants by flocculating them [213].

Rodríguez-Alvarez studied the oxidation effect of permanganate on seven kinds of non-steroidal anti-inflammatory drugs, but only on DCF and indomethacin. The oxidation process was mainly caused by the aromatic ring breaking and the introduction of alcohol and ketone groups, and the highest degradation rate was only 80 % [214]. Zhou found that the presence of MnO₂ in the system could activate Mn (VII) and improve the degradation rate of levofloxacin. When benzoquinone (BQ) was added to the system, the in-situ formation of MnO₂BQ and hydroquinone (HQ) accelerated the reduction of Mn(VII) to MnO₂, significantly increasing the degradation rate [215]. Tuwar conducted experiments on the oxidation of valaciclovir hydrochloride (VCH) by permanganate and found that MnO₄⁻ in potassium permanganate could be complexed with the methylene part of VCH to produce an active substance [MnO₄(OH)]²⁻ to achieve the purpose of VCH degradation [216].

There are very few studies on permanganate degradation of antiviral drugs and immunomodulator drugs. Previous studies on permanganate degradation of pollutants focused on antibiotics and non-steroidal anti-inflammatory drugs. Permanganate plays a decisive role in the effluent quality of WWTP and WTP, especially for antiviral drugs that are difficult to biodegrade. The concentration of drugs in the effluent mainly depends on the removal effect of strong oxidants such as potassium permanganate added in the pretreatment stage. Therefore, in the future, permanganate removal of immunomodulators and antiviral drugs should be further studied.

4.2.1.6. Photocatalysis. Photocatalysis is to activate the catalyst material by light to produce active free radicals to achieve the purpose of degrading pollutants. At the same time, it has the advantages of green environment and no pollution. The •OH, singlet oxygen ¹O₂ and superoxide free radical O₂⁻ are usually produced in the system [217,218].



Where e_{cb}⁻ and h_{vb}⁺ are conduction electron and valence electron vacancy, •OH denotes hydroxyl radical, O₂⁻ denotes superoxide radical.

In the published literature, the mineralization rate of OTV after photocatalysis is < 10 % [70], The mineralization rate of ACV reached 80 %, 3TC > 90 %, AMT reached 91.7 % and zanamivir (ZNV) reached 100 % [219]. Hojamberdiev et al. synthesized WW₃ photocatalyst by calcining waste from the process of making ammonium molybdate [185]. Within 15 min, the removal efficiency of RTV reached 95 %, while LPV needed 60 min of light to achieve the same removal efficiency as RTV. •OH produced in the photocatalytic system would attack the ketone, phenyl and phenoxy structures in LPV, while RTV is cleaved by the hydrolysis of carbamate and urea structures. Wang et al. studied the degradation of IBU and found that the degradation efficiency of IBU would increase with the increase of the concentration in the prepared material. The carrier ZIF-8 in the material inhibited the recombination of electron-hole pairs and increased the number of active sites by dispersing the catalyst [220]. The electron migration is increased, and the photocatalytic activity and degradation efficiency are improved. Studies have shown that O₂ and O₂⁻ are formed at a light intensity of -0.33 eV, and H₂O and •OH are formed at a light intensity of + 0.19 eV [221]. It was confirmed that h⁺ and O₂⁻ were the main active substances in the system. Due to the photostability of some antiviral drugs, the degradation efficiency of some antiviral drugs is not high in the application of photocatalytic degradation. However, some antiviral drugs have aromatic rings in their chemical structure, which can achieve the effect of decomposition by absorbing sunlight [28]. For example, after exposure to light, a single electron in the cyclopropylamine part of the structure of ABC is oxidized and then decomposed to produce small molecules and cyclopropylamine free groups [29]. Under light conditions, •OH will attack the alcohol structure at the end of the ACV structure, and eventually produce aldehydes [222]. In future research, degradation drugs should be selected according to the characteristics of the chemical structure of NCSDs, such as drugs containing aromatic rings, heterocycles, alcohols and other structures, and then degradation by photocatalysis, which will greatly improve the degradation efficiency.

4.2.2. Physical methods

The physical method is a simple operation method, cost-effective water treatment method, compared with the advanced oxidation method and biological method, in the treatment process, greatly reduces the formation of other by-products, and reduce the degradation of pollutants in the environment.

MOFs materials have recently been the focus of research. MOFs is a kind of material with a crystalline porous structure, mainly formed by the connection of metal ions and ion clusters. This network structure is similar to activated carbon and has good adsorption performance. It can be prepared without calcination at ultra-high temperatures, and studies have shown that MOFs can remove antibiotics from water bodies [223]. Viltres et al. prepared Fe-BTB MOF material and studied its adsorption of tetracycline (TC) and sulfamethoxazole (SMZ) in water. The results showed that within 30 min, the adsorption rates of Fe-BTB on TC and SMZ reached 89.4 % and 95.2 %, respectively, and the maximum adsorption capacity reached 649 and 276 mg/g, so most of the pollutants could be adsorbed and removed in a short time [224]. It was also found that the adsorption efficiency of TC was the highest at room temperature. The adsorption rate slightly decreased as the temperature increased, confirming the suitability of Fe-BTB for practical water treatment at room temperature. As shown in Fig. 10, The primary mechanisms for TC and SMZ adsorption include π-π electron donor-acceptor interactions, hydrogen bonding, and electrostatic

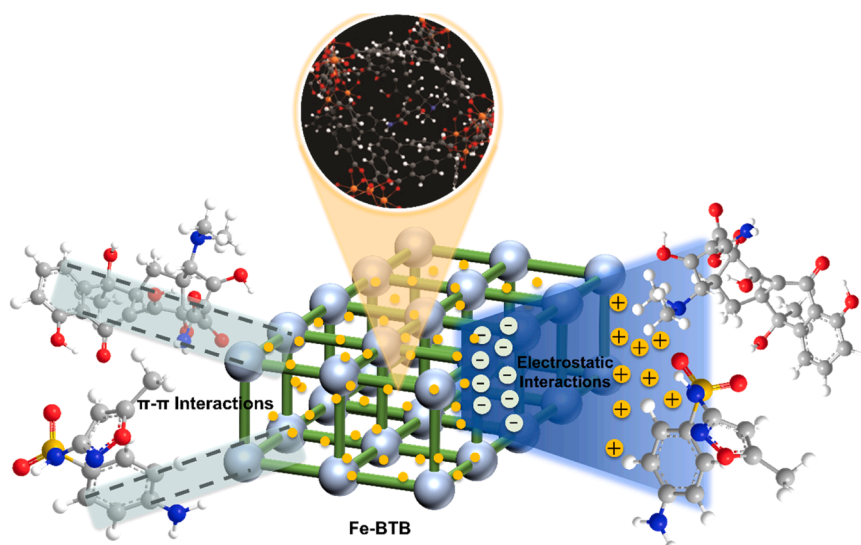


Fig. 10. MOF material adsorption of antiviral drugs [225].

interactions between the aromatic rings in Fe-BTB and the antibiotic molecules, facilitating their adsorption. Even after multiple adsorption-desorption cycles, Fe-BTB retained nearly the same crystallinity as at the outset, highlighting the material's reusability.

Biochar (BC) is another adsorption material, which also has the characteristics of low cost, larger specific surface area and good adsorption effect. Saghir prepared BC @ layered double hydroxide (LDH) composites using pistachio fruit as raw material. LDH nanoparticles were successfully deposited on the surface of BC, and the adsorption capacity of LPV reached 832.9 mg/g [184]. It is reported that the hydroxyl and alkoxy groups present in BC@LDH play a key role in the adsorption of LPV, which may promote the formation of hydrogen bond. At the same time, π - π bond is formed between the benzene ring of LPV and BC@LDH. Under the double action of π - π bond and hydrogen bond, the adsorption effect of LPV is achieved. One of the factors that determine the adsorption capacity of the adsorbent is the type and number of its functional groups, so a single BC may exist because it indicates that the type and number of functional groups are insufficient, resulting in poor adsorption capacity [226]. BC composite material can perfectly solve the problem of an insufficient number of functional groups, and the future will tend to study the adsorption of pollutants in the water environment by BC composite material. At the same time, MOFs material is worth more effort to explore MOFs adsorption material due to its excellent adsorption performance in water treatment. Although there have been studies on the removal of novel coronavirus-specific drugs such as LPV and FPV by adsorption, compared with previous well-known antibiotics, the adsorption of NCSDs in water environment is still worthy of more exploration and discussion.

As shown in Table 5, This study summarizes the cost of different water treatment technologies in practical applications. The selection of an appropriate water treatment technology should be based on a comprehensive evaluation of local economic development levels and the concentration of pollutants in the water. By considering these factors, regions or countries can choose the most suitable technology to maximize the benefits and optimize the cost-effectiveness of water treatment processes.

5. Conclusion and prospects

A review of the literature reveals that water treatment technologies are primarily categorized into biological treatment, advanced oxidation processes, and physical methods. Research on the removal of antibiotics

and non-steroidal anti-inflammatory drugs using these methods is relatively comprehensive and well-developed. This is largely due to the widespread use of antibiotics prior to the COVID-19 outbreak, which occurred in medical treatments, animal husbandry, and various other applications. In China, it is estimated that the Yangtze River receives approximately 3000 tons of antibiotics annually, with detected residues ranging from 2.05 to 111 ng/L [227]. Antiviral drugs constitute a significant portion of NCSDs, but current research on their removal from water predominantly focuses on historical HIV medications. There is a notable lack of studies on the degradation of COVID-19 drugs such as NAT, RDV, MPV, LPV, and FPV. Additionally, immunomodulators, which are widely used in COVID-19 treatment, contribute to the problem. Given the current usage trends and anticipated growth, it is projected that thousands of tons of COVID-19 antivirals could be utilized globally each year by 2030. The presence of NCSDs in the environment poses a considerable risk to ecological health. Therefore, addressing the removal of NCSDs, particularly antiviral drugs, from water is an urgent issue. It is crucial to encourage further research and investment in this area to better manage and mitigate the impact of these substances on aquatic environment.

This study provides a comprehensive summary of the solubility, pKa, LogKow, and other physical and chemical properties, as well as the chemical structures of COVID-19 drugs, enabling subsequent researchers to select appropriate removal technologies. Some antivirals in NCSDs contain nucleotide groups and nucleobase structures, which are particularly vulnerable to attack. For these, removal technologies with strong oxidative potential, such as ferrate, should be employed to effectively degrade these antivirals. Antiviral drugs with a LogKow greater than 3 are more readily adsorbed onto activated sludge, making adsorption or biological methods more effective for their removal. The study also reviewed various removal technologies and found that a combination of multiple methods often yields better results than any single technology alone. Future research should focus on advanced combinations such as bio-advanced oxidation, bio-biological processes, advanced oxidation-advanced oxidation, bio-adsorption, and advanced oxidation-adsorption techniques. While traditional advanced oxidation processes like ozone and UV have been studied for antiviral drug removal, there is limited research on newer oxidants like ferrate and permanganate. Because these substances are highly oxidizing, they are promising candidates for WTP and WWTP. Researchers should further investigate the use of ferrate and permanganate in removing antiviral drugs. Currently, studies on adsorption methods for antiviral and immunomodulator drugs are lacking. Recently, MOFs have gained

Table 5
The cost comparison of COVID-19 drug removal technologies.

Type	Name	Cost	Note
Biological method	Activated sludge process	Low	The activated sludge process is a well-established and widely applied method with relatively low initial investment and operating costs, making it suitable for large-scale water treatment.
	Membrane bioreactor	High	The membrane bioreactor combines activated sludge treatment with membrane filtration technology. While it offers excellent treatment performance, the costs of membranes, maintenance, and higher energy consumption make it relatively expensive.
	Microbial fuel cell	High	Microbial fuel cells are a relatively new technology. Although they offer high energy efficiency and environmental benefits, the initial equipment investment and long economic return period contribute to their high costs.
Non-biological method	Ferrate	Moderately high	Ferrate technology incurs higher costs, particularly for the production of ferrate salts. However, its high efficiency and multifunctional capabilities (such as oxidation and disinfection) offer a cost-effective solution in specific applications.
	Ozonation	Moderate	Ozone generation requires considerable electricity, and the initial capital investment is high. However, ozonation is highly efficient in removing various pollutants and disinfecting water.
	Ultraviolet	Moderately low	The main costs of UV disinfection are related to electricity consumption and equipment investment. However, it does not require chemical agents, and maintenance and operation are relatively simple.
	Electrochemical oxidation	Moderately high	Electrochemical oxidation requires higher initial equipment investment and electricity consumption. However, its effectiveness in degrading pollutants makes it a viable option for high-pollution water treatment.
	Permanganate	Moderate	The use of potassium permanganate involves a significant chemical cost, but the process is straightforward. It is commonly used for the removal of specific pollutants and is effective in some water quality issues.
	Photocatalysis	High	Photocatalysis relies on specific catalysts and ultraviolet light, which involves high material and equipment costs. However, it is highly effective in

Table 5 (continued)

Type	Name	Cost	Note
	Adsorption	Low	degrading organic pollutants and disinfecting water. Adsorption typically utilizes activated carbon or other adsorbent materials (excluding MOF). Although initial costs are relatively low, the need for periodic replacement and regeneration of adsorbents may lead to increased long-term operational costs.

attention due to their excellent adsorption properties and straightforward preparation methods. Utilizing MOFs materials for the removal of coronavirus-specific drugs could offer highly efficient results.

6. Results

In the post-COVID-19 pandemic era, COVID-19 will coexist with human beings for a long time. With the development of drugs, the range of effective drugs for COVID-19 treatment is also shrinking, and such NCSDs will be used for a long time in the future fight against COVID-19, which further increases the risk of environmental harm from NCSDs. In the context of major public health emergencies, water treatment processes are often characterized by the need for achieving efficient treatment outcomes within a short timeframe. Strong oxidants such as ferrate and permanganate play a critical role in ensuring water safety under such circumstances. Compared to the extended timeframes required for biological treatment, the use of ferrate and permanganate in short-term pre-treatment or advanced treatment processes significantly reduces the cost barriers to practical application while ensuring water safety. These oxidants exhibit high efficiency in the removal and inactivation of various emerging contaminants, as well as bacteria and viruses, making them highly suitable for deployment as emergency water treatment agents. Although the existing water treatment technology is very rich, there are still a lot of gaps in the research of NCSDs in the field of environmental science, which need to be explored continuously by researchers, including but not limited to the removal mechanism of NCSDs in the water environment, risk assessment to the environment, and toxicity analysis of by-products generated during removal. The combination of water treatment technology and COVID-19 drugs will also become a research hotspot in the environmental field in the future.

Ethical approval

The authors mentioned in the manuscript have agreed to authorship, read and approved the manuscript and given consent for submission and subsequent publication of the manuscript.

CRediT authorship contribution statement

Yulin Bian: Investigation. **Hyunook Kim:** Writing – review & editing, Software. **Jinfeng Lu:** Investigation. **Cong Li:** Supervision, Project administration, Conceptualization. **Jingzhen Su:** Formal analysis, Data curation. **Zihe Chen:** Writing – review & editing, Writing – original draft, Investigation, Formal analysis, Data curation. **Jiani Xu:** Writing – original draft, Investigation, Formal analysis, Data curation.

Declaration of Competing Interest

The authors declare that they have no known competing financial interests or personal relationships that could have appeared to influence the work reported in this paper.

Acknowledgement

This work was sponsored by the National Natural Science Foundation of China (Project No. 52442006) and Project Sponsored by Science and Technology Commission of Shanghai Municipality (Project No. 24DZ2306400). H. Kim is supported by the Korea Environment Industry & Technology Institute (KEITI) through the project for developing innovative drinking water and wastewater technologies funded by Korea Ministry of Environment (MOE) (NO. 2019002710006) and MOE's Graduate School Specialized in Climate Change.

Appendix A. Supporting information

Supplementary data associated with this article can be found in the online version at [doi:10.1016/j.jece.2025.115310](https://doi.org/10.1016/j.jece.2025.115310).

Data availability

Data will be made available on request.

References

- [1] J. He, T. Feng, L. Tao, Y.-e. Peng, L. Tong, X.-w. Zhao, X. Shao, L.-y. Xu, Y.-l. Yang, Y.-b. Zhao, Distribution and impacts on the geological environment of antiviral drugs in major waters of Wuhan, China, *China Geol.* 5 (2022) 402–410, <https://doi.org/10.31035/cg2022047>.
- [2] Z. Zhang, Y. Zhou, L. Han, X. Guo, Z. Wu, J. Fang, B. Hou, Y. Cai, J. Jiang, Z. Yang, Impacts of COVID-19 pandemic on the aquatic environment associated with disinfection byproducts and pharmaceuticals, *Sci. Total Environ.* 811 (2022) 151409, <https://doi.org/10.1016/j.scitotenv.2021.151409>.
- [3] L. Yao, Z.-Y. Chen, W.-Y. Dou, Z.-K. Yao, X.-C. Duan, Z.-F. Chen, L.-J. Zhang, Y.-J. Nong, J.-L. Zhao, G.-G. Ying, Occurrence, removal and mass loads of antiviral drugs in seven wastewater treatment plants with various treatment processes, *Water Res.* 207 (2021) 117803, <https://doi.org/10.1016/j.watres.2021.117803>.
- [4] Worldometer, 2024. COVID-19 CORONAVIRUS PANDEMIC. (<https://www.worldometers.info/coronavirus/>); (accessed 2 July 2024).
- [5] W.H.O., 2024. WHO COVID-19 dashboard. <https://data.who.int/dashboards/covid19/cases?n=c>; (accessed 14 June 2024).
- [6] W.H.O., 2023. WHO Director-General's opening remarks at the media briefing – 5 May 2023. (<https://www.who.int/director-general/speeches/detail/who-director-general-s-opening-remarks-at-the-media-briefing-5-may-2023>); (accessed 16 May 2024).
- [7] N. Firouzabadi, P. Ghasemiyeh, F. Moradishooli, S. Mohammadi-Samani, Update on the effectiveness of COVID-19 vaccines on different variants of SARS-CoV-2, *Int. Immunopharmacol.* 117 (2023) 109968, <https://doi.org/10.1016/j.intimp.2023.109968>.
- [8] Q. Tan, L. Duan, Y. Ma, F. Wu, Q. Huang, K. Mao, W. Xiao, H. Xia, S. Zhang, E. Zhou, P. Ma, S. Song, Y. Li, Z. Zhao, Y. Sun, Z. Li, W. Geng, Z. Yin, Y. Jin, Is oseltamivir suitable for fighting against COVID-19: in silico assessment, in vitro and retrospective study, *Bioorg. Chem.* 104 (2020) 104257, <https://doi.org/10.1016/j.bioorg.2020.104257>.
- [9] J. Tian, S. Yan, H. Wang, Y. Zhang, Y. Zheng, H. Wu, X. Li, Z. Gao, Y. Ai, X. Gou, L. Zhang, L. He, F. Lian, B. Liu, X. Tong, Hanshiyi Formula, a medicine for Sars-CoV2 infection in China, reduced the proportion of mild and moderate COVID-19 patients turning to severe status: a cohort study, *Pharmacol. Res.* 161 (2020) 105127, <https://doi.org/10.1016/j.phrs.2020.105127>.
- [10] W. Chan, B. He, X. Wang, M.-L. He, Pandemic COVID-19: current status and challenges of antiviral therapies, *Genes Dis.* 7 (2020) 502–519, <https://doi.org/10.1016/j.gendis.2020.07.001>.
- [11] F. Moretto, T. Sixt, H. Devilliers, M. Abdallahoui, I. Eberl, T. Rogier, M. Buisson, P. Chavanet, M. Duong, C. Esteve, S. Mahy, A. Salmon-Rousseau, F. Catherine, M. Blot, L. Piroth, Is there a need to widely prescribe antibiotics in patients hospitalized with COVID-19? *Int. J. Infect. Dis.* 105 (2021) 256–260, <https://doi.org/10.1016/j.ijid.2021.01.051>.
- [12] X. Yang, X. Li, S. Qiu, C. Liu, S. Chen, H. Xia, Y. Zeng, L. Shi, J. Chen, J. Zheng, S. Yang, G. Tian, G. Liu, L. Yang, Global antimicrobial resistance and antibiotic use in COVID-19 patients within health facilities: a systematic review and meta-analysis of aggregated participant data, *J. Infect.* 89 (2024) 106183, <https://doi.org/10.1016/j.jinf.2024.106183>.
- [13] W. Laughey, EPH179 Ibuprofen, other NSAIDs, & COVID-19: a narrative review, *Value Health* 26 (2023) S236, <https://doi.org/10.1016/j.jval.2023.09.1221>.
- [14] R.L. Mitra, S.A. Greenstein, L.M. Epstein, An algorithm for managing QT prolongation in coronavirus disease 2019 (COVID-19) patients treated with either chloroquine or hydroxychloroquine in conjunction with azithromycin: possible benefits of intravenous lidocaine, *Heart Case Rep.* 6 (2020) 244–248, <https://doi.org/10.1016/j.hrcr.2020.03.016>.
- [15] J. Delaleu, B. Deniau, M. Battistella, A. de Masson, B. Bensaid, M. Jachiet, I. Lazaridou, M. Bagot, J.-D. Bouaziz, G. Archer, A. Benattia, A. Bergeron, L. Bondeelle, J.D. Bouaziz, D. Bouda, D. Boutboul, B.I. Brindel, E. Bugnet, S. Caillat Zucman, S. Cassonnet, K. Celli Lebras, J. Chabert, S. Chevret, M. Clément, C. Davoine, N. De Castro, E. De Kerviler, C. De Margerie-Mellon, C. Delaugerre, F. Depret, B. Denis, L. Djaghout, C. Dupin, D. Farge-Bancel, C. Fauvaux, E. Feredj, D. Feyeux, J.P. Fontaine, V. Fremereaux-Bacchi, L. Galicier, S. Harel, J. Al, E. Kozakiewicz, M. Lebel, A. Baye, J. Le Goff, P. Le Guen, E. Lengline, G. Liegeon, G. Lorillon, I. Madelaine Chambrin, G. Martin de Frémont, M. Meunier, J.M. Molina, F. Morin, E. Oksenhendler, R. Peffault de la Tour, O. Peyrony, B. Plaud, M. Salmons, J. Saussereau, J. Soret, Acute generalized exanthematous pustulosis induced by hydroxychloroquine prescribed for COVID-19, *e2771, J. Allergy Clin. Immunol.: Pract.* 8 (2020) 2777–2779, <https://doi.org/10.1016/j.jaip.2020.05.046>.
- [16] L. Manjani, N. Desai, A. Kohli, R. Arya, C. Woods, S. Desale, Effects of acetaminophen on outcomes in patients hospitalized with COVID-19, *Chest* 160 (2021) A1072, <https://doi.org/10.1016/j.chest.2021.07.992>.
- [17] L. Ni, L. Chen, X. Huang, C. Han, J. Xu, H. Zhang, X. Luan, Y. Zhao, J. Xu, W. Yuan, H. Chen, Combating COVID-19 with integrated traditional Chinese and Western medicine in China, *Acta Pharm. Sin. B* 10 (2020) 1149–1162, <https://doi.org/10.1016/j.apsb.2020.06.009>.
- [18] C.K. Kang, M.-W. Seong, S.-J. Choi, T.S. Kim, P.G. Choe, S.H. Song, N.-J. Kim, W. B. Park, M.-d. Oh, In vitro activity of lopinavir/ritonavir and hydroxychloroquine against severe acute respiratory syndrome coronavirus at concentrations achievable by usual doses, *Korean J. Intern. Med.* 35 (2020) 782, <https://doi.org/10.3904/kjim.2020.157>.
- [19] G.o.t.P.s.r.o. China, 2022. Notice on the issuance of the novel coronavirus pneumonia diagnosis and treatment Protocol (trial version 9). (https://www.gov.cn/zhengce/zhengceku/2022-03/15/content_5679257.htm); (accessed 1 July 2024).
- [20] G.o.t.P.s.r.o. China, 2023. Notice on the issuance of diagnosis and treatment Protocol for novel coronavirus infection (trial version 10). (https://www.gov.cn/zhengce/zhengceku/2023-01/06/content_5735343.htm); (accessed 13 May 2024).
- [21] Y. Dian, Y. Meng, Y. Sun, G. Deng, F. Zeng, Azvudine versus Paxlovid for oral treatment of COVID-19 in Chinese patients with pre-existing comorbidities, *J. Infect.* 87 (2023) e24–e27, <https://doi.org/10.1016/j.jinf.2023.05.012>.
- [22] R. Ramachandran, V. Bhosale, H. Reddy, V. Atam, M.M.A. Faridi, J. Fatima, V. Shukla, Z.A. Khan, H. Khan, V. Singh, M.P.S. Negi, M. Srivastava, A. K. Srivastava, C.B. Tripathi, N. Ghosh, N. Majumdar, R.K. Tripathi, S.K. Rath, P. R. Mishra, S. Sharma, T.K. Kundu, Phase III, randomized, double-blind, placebo controlled trial of efficacy, safety and tolerability of antiviral drug umifenovir vs standard care of therapy in non-severe COVID-19 patients, *Int. J. Infect. Dis.* 115 (2022) 62–69, <https://doi.org/10.1016/j.ijid.2021.11.025>.
- [23] R. Gurke, J. Rossmann, S. Schubert, T. Sandmann, M. Rößler, R. Oertel, J. Fauler, Development of a SPE-HPLC-MS/MS method for the determination of most prescribed pharmaceuticals and related metabolites in urban sewage samples, *J. Chromatogr. B* 990 (2015) 23–30, <https://doi.org/10.1016/j.jchromb.2015.03.008>.
- [24] A. Ofrydopoulou, C. Nannou, E. Evgenidou, A. Christodoulou, D. Lambropoulou, Assessment of a wide array of organic micropollutants of emerging concern in wastewater treatment plants in Greece: occurrence, removals, mass loading and potential risks, *Sci. Total Environ.* 802 (2022) 149860, <https://doi.org/10.1016/j.scitotenv.2021.149860>.
- [25] K.O. K'Orege, L. Vergeynst, D. Ombaka, P. De Wispelaere, M. Okoth, H. Van Langenhove, K. Demeester, Occurrence patterns of pharmaceutical residues in wastewater, surface water and groundwater of Nairobi and Kisumu city, Kenya, *Chemosphere* 149 (2016) 238–244, <https://doi.org/10.1016/j.chemosphere.2016.01.095>.
- [26] A.S. Oberoi, Y. Jia, H. Zhang, S.K. Khanal, H. Lu, Insights into the fate and removal of antibiotics in engineered biological treatment systems: a critical review, *Environ. Sci. Technol.* 53 (2019) 7234–7264, <https://doi.org/10.1021/acs.est.9b01131>.
- [27] Z. Guo, H. He, K. Liu, Z. Li, Y. Xi, Z. Liao, G. Dao, B. Huang, X. Pan, Toxic mechanisms of the antiviral drug arbidol on microalgae in algal bloom water at transcriptomic level, *J. Hazard. Mater.* 473 (2024) 134678, <https://doi.org/10.1016/j.jhazmat.2024.134678>.
- [28] C. Nannou, A. Ofrydopoulou, E. Evgenidou, D. Heath, E. Heath, D. Lambropoulou, Antiviral drugs in aquatic environment and wastewater treatment plants: a review on occurrence, fate, removal and ecotoxicity, *Sci. Total Environ.* 699 (2020) 134322, <https://doi.org/10.1016/j.scitotenv.2019.134322>.
- [29] R. Wang, J. Luo, C. Li, J. Chen, N. Zhu, Antiviral drugs in wastewater are on the rise as emerging contaminants: a comprehensive review of spatiotemporal characteristics, removal technologies and environmental risks, *J. Hazard. Mater.* 457 (2023) 131694, <https://doi.org/10.1016/j.jhazmat.2023.131694>.
- [30] M. Kumar, K. Kuroda, K. Dhangar, P. Mazumder, C. Sonne, J. Rinklebe, M. Kitajima, Potential emergence of antiviral-resistant pandemic viruses via environmental drug exposure of animal reservoirs, *Environ. Sci. Technol.* 54 (2020) 8503–8505, <https://doi.org/10.1021/acs.est.0c03105>.
- [31] C. Lopes, S. Charles, B. Vollat, J. Garric, Toxicity of ivermectin on cladocerans: comparison of toxic effects on daphnia and ceriodaphnia species, *Environ. Toxicol. Chem.* 28 (2009) 2160–2166, <https://doi.org/10.1897/08-607.1>.
- [32] N. Schweitzer, G. Fink, T.A. Ternes, K. Duis, Effects of ivermectin-spiked cattle dung on a water-sediment system with the aquatic invertebrates *Daphnia magna* and *Chironomus riparius*, *Aquat. Toxicol.* 97 (2010) 304–313, <https://doi.org/10.1016/j.aquatox.2009.12.017>.
- [33] I.M. Tleyjeh, Z. Kashour, O. Aldosary, M. Riaz, H. Tlayjeh, M.A. Garbati, R. Tleyjeh, M.H. Al-Mallah, M.R. Sohail, D. Gerberi, A.A. Bin Abdulhak, J. R. Giudicessi, M.J. Ackerman, T. Kashour, Cardiac toxicity of chloroquine or

- hydroxychloroquine in patients with COVID-19: a systematic review and meta-regression analysis, *Mayo Clin. Proc.: Innov., Qual. Outcomes* 5 (2021) 137–150, <https://doi.org/10.1016/j.mayocpico.2020.10.005>.
- [34] P. Ruamviboonsuk, T.Y.Y. Lai, A. Chang, C.-C. Lai, W.F. Mieler, D.S.C. Lam, Chloroquine and hydroxychloroquine retinal toxicity consideration in the treatment of COVID-19, *Asia-Pacific, J. Ophthalmol.* 9 (2020) 85–87, <https://doi.org/10.1097/APO.0000000000000289>.
- [35] V. Desgens-Martin, A.A. Keller, COVID-19 treatment agents: do they pose an environmental risk, *ACS Est. Water* 1 (2021) 1555–1565, <https://doi.org/10.1021/acsestwater.1c00059>.
- [36] Z. Chen, X. Zhao, Y. Li, R. Zhang, Z. Nie, X. Cheng, X. Zhang, H. Wang, Course-, dose-, and stage-dependent toxic effects of prenatal dexamethasone exposure on long bone development in fetal mice, *Toxicol. Appl. Pharmacol.* 351 (2018) 12–20, <https://doi.org/10.1016/j.taap.2018.05.005>.
- [37] Y. Chen, D. Xu, X. Xia, G. Chen, H. Xiao, L. Chen, H. Wang, Sex difference in adrenal developmental toxicity induced by dexamethasone and its intrauterine programming mechanism, *Pharmacol. Res.* 174 (2021) 105942, <https://doi.org/10.1016/j.phrs.2021.105942>.
- [38] K. Kuroda, C. Li, K. Dhangar, M. Kumar, Predicted occurrence, ecotoxicological risk and environmentally acquired resistance of antiviral drugs associated with COVID-19 in environmental waters, *Sci. Total Environ.* 776 (2021), <https://doi.org/10.1016/j.scitotenv.2021.145740>.
- [39] A. Gunaydin-Akyildiz, N. Aksoy, T. Boran, E.N. Ilhan, G. Ozhan, Favipiravir induces oxidative stress and genotoxicity in cardiac and skin cells, *Toxicol. Lett.* 371 (2022) 9–16, <https://doi.org/10.1016/j.toxlet.2022.09.011>.
- [40] L. Boulard, G. Dierkes, T. Ternes, Utilization of large volume zwitterionic hydrophilic interaction liquid chromatography for the analysis of polar pharmaceuticals in aqueous environmental samples: benefits and limitations, *J. Chromatogr. A* 1535 (2018) 27–43, <https://doi.org/10.1016/j.chroma.2017.12.023>.
- [41] A. Ripanda, M.J. Rwiza, E.C. Nyanza, R. Bakari, H. Miraji, K.N. Njau, S.A. Hamad Vuai, R.L. Machunda, Removal of lamivudine from synthetic solution using jamun seed (*Syzygium cumini*) biochar adsorbent, *Emerg. Contam.* 9 (2023) 100232, <https://doi.org/10.1016/j.emcon.2023.100232>.
- [42] O.A. Abafe, J. Späth, J. Fick, S. Jansson, C. Buckley, A. Stark, B. Pietruschka, B. S. Martincigh, LC-MS/MS determination of antiretroviral drugs in influents and effluents from wastewater treatment plants in KwaZulu-Natal, South Africa, *Chemosphere* 200 (2018) 660–670, <https://doi.org/10.1016/j.chemosphere.2018.02.105>.
- [43] A. Fresse, D. Viard, S. Romani, A. Gérard, M. Lepelle, F. Rocher, J.-E. Salem, M.-D. Drici, Spontaneous reported cardiotoxicity induced by lopinavir/ritonavir in COVID-19. An alleged past-resolved problem, *Int. J. Cardiol.* 324 (2021) 255–260, <https://doi.org/10.1016/j.ijcard.2020.10.028>.
- [44] C. Prasse, M.P. Schluessener, R. Schulz, T.A. Ternes, Antiviral drugs in wastewater and surface waters: a new pharmaceutical class of environmental relevance, *Environ. Sci. Technol.* 44 (2010) 1728–1735, <https://doi.org/10.1021/es903216p>.
- [45] R. Nugnes, E. Orlo, C. Russo, M. Lavorgna, M. Isidori, Comprehensive eco-genotoxicity and environmental risk of common antiviral drugs in aquatic environments post-pandemic, *J. Hazard. Mater.* 480 (2024) 135947, <https://doi.org/10.1016/j.jhazmat.2024.135947>.
- [46] Y. Aminot, X. Litrico, M. Chambolle, C. Arnaud, P. Pardon, H. Budzinski, Development and application of a multi-residue method for the determination of 53 pharmaceuticals in water, sediment, and suspended solids using liquid chromatography-tandem mass spectrometry, -8623, *Anal. Bioanal. Chem.* 407 (2015) 8623, <https://doi.org/10.1007/s00216-015-9095-2>.
- [47] Y. Gu, J. Huang, G. Zeng, L. Shi, Y. Shi, K. Yi, Fate of pharmaceuticals during membrane bioreactor treatment: status and perspectives, *Bioresour. Technol.* 268 (2018) 733–748, <https://doi.org/10.1016/j.biortech.2018.08.029>.
- [48] E. Sahar, R. Messalem, H. Cikurel, A. Aharoni, A. Brenner, M. Godehardt, M. Jekel, M. Ernst, Fate of antibiotics in activated sludge followed by ultrafiltration (CAS-UF) and in a membrane bioreactor (MBR), *Water Res.* 45 (2011) 4827–4836, <https://doi.org/10.1016/j.watres.2011.06.023>.
- [49] M.E. Mohadab, B. Bouikhalene, S. Safi, Bibliometric method for mapping the state of the art of scientific production in Covid-19, *Chaos Solitons Fractals* 139 (2020) 110052, <https://doi.org/10.1016/j.chaos.2020.110052>.
- [50] G. Chen, S. Hong, C. Du, P. Wang, Z. Yang, L. Xiao, Comparing semantic representation methods for keyword analysis in bibliometric research, *J. Informetr.* 18 (2024) 101529, <https://doi.org/10.1016/j.joi.2024.101529>.
- [51] W.H.O.2024. Number of COVID-19 cases reported to WHO (cumulative total). (<https://data.who.int/dashboards/covid19/cases?n=c>); (accessed 17 June 2024).
- [52] S.P. Rautenbach, L.K. Whittles, G. Meyer-Rath, L. Jamieson, T. Chidirikire, L. F. Johnson, J.W. Imai-Eaton, Future HIV epidemic trajectories in South Africa and projected long-term consequences of reductions in general population HIV testing: a mathematical modelling study, *Lancet Public Health* 9 (2024) e218–e230, [https://doi.org/10.1016/S2468-2667\(24\)00020-3](https://doi.org/10.1016/S2468-2667(24)00020-3).
- [53] D. Russo, A. Siciliano, M. Guida, E. Galdiero, A. Amoresano, R. Andreozzi, N. M. Reis, G. Li Puma, R. Marotta, Photodegradation and ecotoxicology of acyclovir in water under UV254 and UV254/H2O2 processes, *Water Res.* 122 (2017) 591–602, <https://doi.org/10.1016/j.watres.2017.06.020>.
- [54] Z. Guo, H. He, K. Liu, S. Yang, Z. Li, C. Lai, Z. Liao, X. Ren, B. Huang, X. Pan, Sunlight-induced degradation of COVID-19 antivirals arbidol in natural aquatic environments: mechanisms, pathways and toxicity, *J. Environ. Manag.* 347 (2023) 119113, <https://doi.org/10.1016/j.jenvman.2023.119113>.
- [55] Z. Liu, F. Liang, S. Gao, X. Zhu, X. Song, W. Chen, X. Tao, Z. Wang, D. Xu, Separation and quantification of Azvudine in plasma of patients with COVID-19 using LC-MS/MS, *J. Pharm. Biomed. Anal.* 236 (2023) 115736, <https://doi.org/10.1016/j.jpba.2023.115736>.
- [56] V.F. Samanidou, E.N. Evaggelopoulou, I.N. Papadopyannis, Simultaneous determination of quinine and chloroquine anti-malarial agents in pharmaceuticals and biological fluids by HPLC and fluorescence detection, *J. Pharm. Biomed. Anal.* 38 (2005) 21–28, <https://doi.org/10.1016/j.jpba.2004.12.005>.
- [57] T. Azuma, M. Ishida, K. Hisamatsu, A. Yunoki, K. Otomo, M. Kunitou, M. Shimizu, K. Hosomaru, S. Mikata, Y. Mino, Fate of new three anti-influenza drugs and one prodrug in the water environment, *Chemosphere* 169 (2017) 550–557, <https://doi.org/10.1016/j.chemosphere.2016.11.102>.
- [58] D. Shyamala, Ashok, Method development and validation of degradation studies of favipiravir by RP-HPLC, *J. Pharm. Res. Int.* 33 (2021) 220–228, <https://doi.org/10.9734/JPRI/2021/v33i42A32399>.
- [59] I. Bulduk, HPLC-UV method for quantification of favipiravir in pharmaceutical formulations, *Acta Chromatogr.* 33 (2021) 209–215, <https://doi.org/10.1556/1326.2020.00828>.
- [60] J. Peluso, F. Gamarra, C.M. Aronson, Synergistic interactions between the emerging contaminant ivermectin and the ubiquitous pesticide glyphosate at an environmentally relevant ratio on *Rhinella arenarum* larvae, *Chemosphere* 358 (2024) 142058, <https://doi.org/10.1016/j.chemosphere.2024.142058>.
- [61] J. Raich-Montiu, K.A. Krogh, M. Granados, J.A. Joensson, B. Halling-Sorensen, Determination of ivermectin and transformation products in environmental waters using hollow fibre-supported liquid membrane extraction and liquid chromatography-mass spectrometry/mass spectrometry, *J. Chromatogr. A* 1187 (2008) 275–280, <https://doi.org/10.1016/j.chroma.2008.02.063>.
- [62] S.R. Chitturi, C. Bharathi, A.V.R. Reddy, K.C. Reddy, H.K. Sharma, V.K. Handa, R. Dandala, V.H. Bindu, Impurity profile study of lopinavir and validation of HPLC method for the determination of related substances in lopinavir drug substance, *J. Pharm. Biomed. Anal.* 48 (2008) 1430–1440, <https://doi.org/10.1016/j.jpba.2008.09.015>.
- [63] M. Galaburda, M. Nazarkovsky, K. Osipiuk, B. Czech, M.V. Borysenko, A. Gladysz-Plaska, A. Lipke, B.A. Marinkovic, R.C.S. Navarro, A. Derylo-Marczewska, Enhanced photocatalytic degradation of antiviral drugs lopinavir and ritonavir by Ni doped ZnO/SiO₂ nanocomposites, *J. Environ. Chem. Eng.* 12 (2024) 114525, <https://doi.org/10.1016/j.jece.2024.114525>.
- [64] H.A. Wagdy, A newly developed and validated environmentally friendly RP-HPLC stability indicating method for the COVID-19 antiviral Molnupiravir: application to degradation kinetics structure suggestion using LC-MS and the effect on viable cells of the major degradation products, *Microchem. J.* 199 (2024) 109980, <https://doi.org/10.1016/j.microc.2024.109980>.
- [65] S. Jain, S. Giri, N. Sharma, R.P. Shah, LC and LC-HRMS studies on stability behavior of molnupiravir an anti-COVID 19 drug, *J. Liq. Chromatogr. Relat. Technol.* 44 (2021) 750–759, <https://doi.org/10.1080/10826076.2022.2063331>.
- [66] E. Dailly, F. Raffi, P. Jolliet, Determination of atazanavir and other antiretroviral drugs (indinavir, amprenavir, nelfinavir and its active metabolite M8, saquinavir, ritonavir, lopinavir, nevirapine and efavirenz) plasma levels by high performance liquid chromatography with UV detection, *J. Chromatogr. B* 813 (2004) 353–358, <https://doi.org/10.1016/j.jchromb.2004.10.005>.
- [67] T.P. Wood, A.E. Basson, C. Duvenage, E.R. Rohwer, The chlorination behaviour and environmental fate of the antiretroviral drug nevirapine in South African surface water, *Water Res.* 104 (2016) 349–360, <https://doi.org/10.1016/j.watres.2016.08.038>.
- [68] S.I. Aboras, H.M. Maher, Green adherent degradation kinetics study of Nirmatrelvir, an oral anti-COVID-19: characterization of degradation products using LC-MS with insilico toxicity profile, *Bmc Chem.* 17 (2023), <https://doi.org/10.1186/s13065-023-00928-z>.
- [69] P. Alegety, S. Byreddy, Development of a novel quality by design-enabled stability-indicating HPLC method and its validation for the quantification of nirmatrelvir in bulk and pharmaceutical dosage forms, *Biomed. Chromatogr.* 38 (2024), <https://doi.org/10.1002/bmc.5812>.
- [70] W.-L. Wang, Q.-Y. Wu, Z.-M. Wang, H.-Y. Hu, N. Negishi, M. Torimura, Photocatalytic degradation of the antiviral drug Tamiflu by UV-A/TiO₂: Kinetics and mechanisms, *Chemosphere* 131 (2015) 41–47, <https://doi.org/10.1016/j.chemosphere.2015.02.032>.
- [71] A. Gupta, S. Guttikar, P.S. Shrivastav, M. Sanyal, Simultaneous quantification of prodrug oseltamivir and its metabolite oseltamivir carboxylate in human plasma by LC-MS/MS to support a bioequivalence study, *J. Pharm. Anal.* 3 (2013) 149–160, <https://doi.org/10.1016/j.jpba.2012.11.004>.
- [72] R. Nguyen, J.C. Goodell, P.S. Shankarappa, S. Zimmerman, T. Yin, C.J. Peer, W. D. Figg, Development and validation of a simple, selective, and sensitive LC-MS/MS assay for the quantification of remdesivir in human plasma, *J. Chromatogr. B* 1171 (2021) 122641, <https://doi.org/10.1016/j.jchromb.2021.122641>.
- [73] A.E. Ibrahim, S.E. Deeb, E.M. Abdelhalim, A. Al-Harasi, R.A. Sayed, Green stability indicating organic solvent-free HPLC determination of remdesivir in substances and pharmaceutical dosage forms, *Separations* 8 (2021), <https://doi.org/10.3390/separations8120243>.
- [74] Z. Li, C. Wu, Q. Zheng, J. Yang, L. Yang, H. sun, C. Liu, W. Zhang, Y. Zheng, K. Cai, Accelerated degradation and toxicity reduction of ribavirin by organic free radicals in the ferrate-acetylacetonate system, *Sep. Purif. Technol.* 330 (2024) 125636, <https://doi.org/10.1016/j.seppur.2023.125636>.
- [75] H. van der Lijke, J.-W.C. Alffenaar, W.T. Kok, B. Greijdanus, D.R.A. Uges, Determination of ribavirin in human serum using liquid chromatography tandem mass spectrometry, *Talanta* 88 (2012) 385–390, <https://doi.org/10.1016/j.talanta.2011.11.004>.

- [76] R.N. Rao, B. Ramachandra, R.M. Vali, S.S. Raju, LC-MS/MS studies of ritonavir and its forced degradation products, *J. Pharm. Biomed. Anal.* 53 (2010) 833–842, <https://doi.org/10.1016/j.jpba.2010.06.004>.
- [77] M. Kurmi, A. Sahu, S.K. Tiwari, S. Singh, Stability behaviour of antiretroviral drugs and their combinations. 6: evidence of formation of potentially toxic degradation products of zidovudine under hydrolytic and photolytic conditions, *Rsc Adv.* 7 (2017) 18803–18814, <https://doi.org/10.1039/c7ra00678k>.
- [78] J. Funke, C. Prasse, C. Dietrich, T.A. Ternes, Ozonation products of zidovudine and thymidine in oxidative water treatment, *Water Res.* X 11 (2021) 100090, <https://doi.org/10.1016/j.wroa.2021.100090>.
- [79] T. Reçber, S.S. Timur, S. Erdoğan Kablan, F. Yağcı, T.C. Karabulut, R. Neslihan Gürsoy, H. Eroğlu, S. Kir, E. Nemutlu, A stability indicating RP-HPLC method for determination of the COVID-19 drug molnupiravir applied using nanoformulations in permeability studies, *J. Pharm. Biomed. Anal.* 214 (2022) 114693, <https://doi.org/10.1016/j.jpba.2022.114693>.
- [80] J.A. Dijkstra, M.G.G. Sturkenboom, K. van Hateren, R.A. Koster, B. Greijdanus, J.-W.C. Alffenaar, Quantification of amikacin and kanamycin in serum using a simple and validated LC-MS/MS method, *Bioanalysis* 6 (2014) 2125–2133, <https://doi.org/10.4155/bio.14.191>.
- [81] G. Hoizey, D. Lamiable, C. Frances, T. Trenque, M. Kaltenbach, J. Denis, H. Millart, Simultaneous determination of amoxicillin and clavulanic acid in human plasma by HPLC with UV detection, *J. Pharm. Biomed. Anal.* 30 (2002) 661–666, [https://doi.org/10.1016/S0731-7085\(02\)00289-3](https://doi.org/10.1016/S0731-7085(02)00289-3).
- [82] R. Deepika, M.G. Sethuraman, Unravelling the efficacy of pencil graphite anode decorated with PdCu@ γ -Fe₂O₃ nanoparticles in the electro-oxidation of amoxicillin: Insights into kinetics, oxidative pathways and toxicity evaluation, *J. Water Process Eng.* 64 (2024) 105651, <https://doi.org/10.1016/j.jpwe.2024.105651>.
- [83] Z.Y. Yang, L. Wang, X. Tang, Determination of azithromycin by ion-pair HPLC with UV detection, *J. Pharm. Biomed. Anal.* 49 (2009) 811–815, <https://doi.org/10.1016/j.jpba.2008.12.018>.
- [84] M.Rosa Boleda, E. Alechaga, E. Moyano, M.Teresa Galceran, F. Ventura, Survey of the occurrence of pharmaceuticals in Spanish finished drinking waters, *Environ. Sci. Pollut. Res.* 21 (2014) 10917–10939, <https://doi.org/10.1007/s11356-014-2885-9>.
- [85] Y. Ni, Y. Kang, Y. Liu, F. Liu, W. Bi, J. Qin, Y. Wu, Z. Sun, Fabrication and characterizations of a novel Ce modified PbO₂ electrode with Ti4O7-rGO as the middle layer for degradation of cefazidime, *Desalination* 582 (2024) 117645, <https://doi.org/10.1016/j.desal.2024.117645>.
- [86] P. Duan, X. Yang, G. Huang, J. Wei, Z. Sun, X. Hu, La₂O₃-CuO₂/CNTs electrode with excellent electrocatalytic oxidation ability for cefazidime removal from aqueous solution, *Colloids Surf. A-Physicochem. Eng. Asp.* 569 (2019) 119–128, <https://doi.org/10.1016/j.colsurfa.2019.02.056>.
- [87] M.A. Akl, M.A. Ahmed, A. Ramadan, Validation of an HPLC-UV method for the determination of ceftriaxone sodium residues on stainless steel surface of pharmaceutical manufacturing equipments, *J. Pharm. Biomed. Anal.* 55 (2011) 247–252, <https://doi.org/10.1016/j.jpba.2011.01.020>.
- [88] K. Elgendy, M. Zaky, T. Alaa Eldin, S. Fadel, Rapid HPLC determination of ciprofloxacin, ofloxacin, and marbofloxacin alone or in a mixture, *Results Chem.* 5 (2023) 100749, <https://doi.org/10.1016/j.rechem.2022.100749>.
- [89] D. Quoc Tuc, F. Alliot, E. Moreau-Guigon, J. Eurin, M. Chevreuil, P. Labadie, Measurement of trace levels of antibiotics in river water using on-line enrichment and triple-quadrupole LC-MS/MS, *Talanta* 85 (2011) 1238–1245, <https://doi.org/10.1016/j.talanta.2011.05.013>.
- [90] M. Lalitha Devi, K.B. Chandrasekhar, A validated stability-indicating RP-HPLC method for levofloxacin in the presence of degradation products, its process related impurities and identification of oxidative degradant, *J. Pharm. Biomed. Anal.* 50 (2009) 710–717, <https://doi.org/10.1016/j.jpba.2009.05.038>.
- [91] H. Wei, J. Li, K.-B. Li, J.-Y. Sun, F. Zhao, Effect of CCl₄ on antibiotics levofloxacin's ultrasonic degradation, *Chem. J. Chin. Univ.* -Chin. 33 (2012) 1438–1443, <https://doi.org/10.3969/j.issn.0251-0790.2012.07.013>.
- [92] D. Fage, G. Deprez, B. Fontaine, F. Wolff, F. Cotton, Simultaneous determination of 8 beta-lactams and linezolid by an ultra-performance liquid chromatography method with UV detection and cross-validation with a commercial immunoassay for the quantification of linezolid, *Talanta* 221 (2021) 121641, <https://doi.org/10.1016/j.talanta.2020.121641>.
- [93] R. Denooz, C. Charlier, Simultaneous determination of five β -lactam antibiotics (cefepim, ceftazidim, cefuroxime, meropenem and piperacillin) in human plasma by high-performance liquid chromatography with ultraviolet detection, *J. Chromatogr. B* 864 (2008) 161–167, <https://doi.org/10.1016/j.jchromb.2008.01.037>.
- [94] A. Ahmadi, B. Vogler, Y. Deng, T. Wu, Removal of meropenem from environmental matrices by electrochemical oxidation using Co/Bi/TiO₂ nanotube electrodes, *Environ. Sci. -Water Res. Technol.* 6 (2020) 2197–2208, <https://doi.org/10.1039/d0ew00184h>.
- [95] D. Sirok, M. Pátfalusi, G. Szelezky, G. Somorjai, D. Greskovits, K. Monostory, Robust and sensitive LC/MS-MS method for simultaneous detection of acetylsalicylic acid and salicylic acid in human plasma, *Microchem. J.* 136 (2018) 200–208, <https://doi.org/10.1016/j.microc.2016.11.005>.
- [96] M. Farah, J. Giralt, F. Stüber, J. Font, A. Fabregat, A. Fortuny, Intensification of diclofenac removal through supported liquid membrane and ozonation, *Environ. Technol. Innov.* 33 (2024) 103469, <https://doi.org/10.1016/j.eti.2023.103469>.
- [97] B.X. Mayer, K. Namirani, P. Dehghanyar, R. Stroh, H. Mascher, M. Müller, Comparison of UV and tandem mass spectrometric detection for the high-performance liquid chromatographic determination of diclofenac in microdialysis samples, *J. Pharm. Biomed. Anal.* 33 (2003) 745–754, [https://doi.org/10.1016/S0731-7085\(03\)00301-7](https://doi.org/10.1016/S0731-7085(03)00301-7).
- [98] N.A. Jayalatha, C.P. Devatha, Experimental investigation for treating ibuprofen and triclosan by biosurfactant from domestic wastewater, *J. Environ. Manag.* 328 (2023) 116913, <https://doi.org/10.1016/j.jenvman.2022.116913>.
- [99] M. Vavrova, P. Landova, T. Svestkova, J. Buresova, Determination of ibuprofen and diclofenac in surface waters by LC-MS-MS, *Chem. Listy* 112 (2018) 329–332, <https://doi.org/10.1556/1326.2022.01089>.
- [100] F. Temussi, F. Cermola, M. DellaGreca, M.R. Iesce, M. Passananti, L. Previtera, A. Zarrelli, Determination of photostability and photodegradation products of indomethacin in aqueous media, *J. Pharm. Biomed. Anal.* 56 (2011) 678–683, <https://doi.org/10.1016/j.jpba.2011.07.005>.
- [101] X.S. Miao, B.G. Koenig, C.D. Metcalfe, Analysis of acidic drugs in the effluents of sewage treatment plants using liquid chromatography-electrospray ionization tandem mass spectrometry, *J. Chromatogr. A* 952 (2002) 139–147, [https://doi.org/10.1016/S0021-9673\(02\)00088-2](https://doi.org/10.1016/S0021-9673(02)00088-2).
- [102] O. Vozniuk, Z. Kejik, K. Vesela, M. Skalickova, P. Novotny, R. Hromadka, J. Hajdud, P. Martasek, M. Jakubek, A fast HPLC/UV method for determination of ketoprofen in cellular media, *Chemistryopen* 13 (2024), <https://doi.org/10.1002/open.202300147>.
- [103] J.B. Quintana, S. Weiss, T. Reemtsma, Pathways and metabolites of microbial degradation of selected acidic pharmaceutical and their occurrence in municipal wastewater treated by a membrane bioreactor, *Water Res.* 39 (2005) 2654–2664, <https://doi.org/10.1016/j.watres.2005.04.068>.
- [104] G. Xu, M. Li, Y. Wang, N. Zheng, L. Yang, H. Yu, Y. Yu, A novel Ag-BiOBr-rGO photocatalyst for enhanced ketoprofen degradation: kinetics and mechanisms, *Sci. Total Environ.* 678 (2019) 173–180, <https://doi.org/10.1016/j.scitotenv.2019.04.418>.
- [105] M. Jiménez-Salcedo, M. Monge, M.T. Tena, The photocatalytic degradation of naproxen with g-C₃N₄ and visible light: identification of primary by-products and mechanism in tap water and ultrapure water, *J. Environ. Chem. Eng.* 10 (2022) 106964, <https://doi.org/10.1016/j.jece.2021.106964>.
- [106] T. Ding, K. Lin, B. Yang, M. Yang, J. Li, W. Li, J. Gan, Biodegradation of naproxen by freshwater algae *Cymbella* sp. and *Scenedesmus quadricauda* and the comparative toxicity, *Bioresour. Technol.* 238 (2017) 164–173, <https://doi.org/10.1016/j.biortech.2017.04.018>.
- [107] A. Abdelhaleem, H.N. Abdelhamid, M.G. Ibrahim, W. Chu, Photocatalytic degradation of paracetamol using photo-Fenton-like metal-organic framework-derived CuO/C under visible LED, *J. Clean. Prod.* 379 (2022) 134571, <https://doi.org/10.1016/j.jclepro.2022.134571>.
- [108] N.H. El Najjar, A. Touffet, M. Deborde, R. Journal, N.K.V. Leitner, Kinetics of paracetamol oxidation by ozone and hydroxyl radicals, formation of transformation products and toxicity, *Sep. Purif. Technol.* 136 (2014) 137–143, <https://doi.org/10.1016/j.seppur.2014.09.004>.
- [109] M.A. Mohamed, Validated stability indicating chromatographic method for determination of baricitinib and its degradation products in their tablet dosage form: Implementation to content uniformity and in vitro dissolution studies, *Ann. Pharm. Françaises* 81 (2023) 267–283, <https://doi.org/10.1016/j.pharma.2022.09.001>.
- [110] S. Veerarahgavan, S.R.S. Thappali, S. Viswanadha, S. Vakkalanka, M. Rangaswamy, Simultaneous quantification of baricitinib and methotrexate in rat plasma by LC-MS/MS: application to a pharmacokinetic study, *Sci. Pharm.* 84 (2016) 347–359, <https://doi.org/10.3797/scipharm.1510-08>.
- [111] A.L. Zayed, G.N. Hamadneh, J.A. Hroot, A. Mayyas, S.A. Jaber, N.A. Qinna, HPLC methods for studying pharmacokinetics of tirozani and in vitro metabolic interaction with dexamethasone in rat, *J. Pharm. Biomed. Anal.* 232 (2023) 115423, <https://doi.org/10.1016/j.jpba.2023.115423>.
- [112] A.V. Quaresma, K.T.S. Rubio, J.G. Taylor, B.A. Sousa, S.Q. Silva, A.A. Werle, R.J. C.F. Afonso, Removal of dexamethasone by oxidative processes: structural characterization of degradation products and estimation of the toxicity, *J. Environ. Chem. Eng.* 9 (2021) 106884, <https://doi.org/10.1016/j.jece.2021.106884>.
- [113] D. Yeniceci, D. Dogrukul-Ak, M. Tuncel, Determination of leflunomide in tablets by high performance liquid chromatography, *J. Pharm. Biomed. Anal.* 40 (2006) 197–201, <https://doi.org/10.1016/j.jpba.2005.06.030>.
- [114] B. Cao, G. He, H. Yang, H. Chang, S. Li, A. Deng, Development of a highly sensitive and specific enzyme-linked immunosorbent assay (ELISA) for the detection of phenylethanolamine A in tissue and feed samples and confirmed by liquid chromatography tandem mass spectrometry (LC-MS/MS), *Talanta* 115 (2013) 624–630, <https://doi.org/10.1016/j.talanta.2013.06.026>.
- [115] PubChem, 2024. COMPOUND SUMMARY. <https://pubchem.ncbi.nlm.nih.gov/>; (accessed 28 August 2024).
- [116] ChemSpider, 2024. Search ChemSpider. <https://www.chemspider.com/Default.aspx>; (accessed 8 August 2024).
- [117] EPA, 2024. U.S. Environmental Protection Agency. (<https://www.epa.gov/>); (accessed 8 July 2024).
- [118] A. Dagens, L. Sigfrid, E. Cai, S. Lipworth, V. Cheung, E. Harris, P. Bannister, I. Rigby, P. Horby, Scope, quality, and inclusivity of clinical guidelines produced early in the covid-19 pandemic: rapid review, *Bmj-Br. Med. J.*, 369 (2020), <https://doi.org/10.1136/bmj.m1936>.
- [119] M.-J. Yang, L. Jiang, L. Xu, S.-L. Guo, Association between paxlovid and mortality rates in critically ill patients with COVID-19 receiving invasive mechanical ventilation: a retrospective cohort study, *Chest* 165 (2024) 128–131, <https://doi.org/10.1016/j.chest.2023.07.012>.
- [120] C.K.H. Wong, I.C.H. Au, K.T.K. Lau, E.H.Y. Lau, B.J. Cowling, G.M. Leung, Real-world effectiveness of molnupiravir and nirmatrelvir plus ritonavir against

- mortality, hospitalisation, and in-hospital outcomes among community-dwelling, ambulatory patients with confirmed SARS-CoV-2 infection during the omicron wave in Hong Kong: an observational study, *Lancet* 400 (2022) 1213–1222, [https://doi.org/10.1016/S0140-6736\(22\)01586-0](https://doi.org/10.1016/S0140-6736(22)01586-0).
- [121] N. Sakander, A. Ahmed, M. Bhardwaj, D. Kumari, U. Nandi, D. Mukherjee, A path from synthesis to emergency use authorization of molnupiravir as a COVID-19 therapy, *Bioorg. Chem.* 147 (2024) 107379, <https://doi.org/10.1016/j.bioorg.2024.107379>.
- [122] E.K. McCreary, J.M. Pogue, Coronavirus disease 2019 treatment: a review of early and emerging options, -ofaa105, *Open Forum Infect. Dis.* 7 (2020) ofaa105, <https://doi.org/10.1093/ofid/ofaa105>.
- [123] J.C. Gallagher, R.L. Morgan, Successful immunomodulators for the treatment of COVID-19 have opened the pathway for comparative trials, *Clin. Microbiol. Infect.* 29 (2023) 7–9, <https://doi.org/10.1016/j.cmi.2022.10.016>.
- [124] M. Bektaş, M. Ay, M. Hamdi Uyar, M. İbkal Kılıç, Combination therapy of high-dose intravenous anakinra and baricitinib in patients with critical COVID-19: promising results from retrospective observational study, *Int. Immunopharmacol.* 129 (2024) 111586, <https://doi.org/10.1016/j.intimp.2024.111586>.
- [125] J. Liu, X. Zheng, Y. Huang, H. Shan, J. Huang, Successful use of methylprednisolone for treating severe COVID-19, *J. Allergy Clin. Immunol.* 146 (2020) 325–327, <https://doi.org/10.1016/j.jaci.2020.05.021>.
- [126] J. Li, R. Gao, G. Wu, X. Wu, Z. Liu, H. Wang, Y. Huang, Z. Pan, J. Chen, X. Wu, Clinical characteristics of emergency surgery patients infected with coronavirus disease 2019 (COVID-19) pneumonia in Wuhan, China, *Surgery* 168 (2020) 398–403, <https://doi.org/10.1016/j.surg.2020.05.007>.
- [127] J. Qiao, What are the risks of COVID-19 infection in pregnant women, *Lancet* 395 (2020) 760–762, [https://doi.org/10.1016/S0140-6736\(20\)30365-2](https://doi.org/10.1016/S0140-6736(20)30365-2).
- [128] G.A. Fitzgerald, Misguided drug advice for COVID-19, -1434, *Science* 367 (2020) 1434, <https://doi.org/10.1126/science.abb8034>.
- [129] X.-T. Shao, Y.-S. Wang, Z.-F. Gong, Y.-Y. Li, D.-Q. Tan, J.-G. Lin, W. Pei, D.-G. Wang, Surveillance of COVID-19 and influenza A(H1N1) prevalence in China via medicine-based wastewater biomarkers, *Water Res.* 247 (2023), <https://doi.org/10.1016/j.watres.2023.120783>.
- [130] F. Zhou, T. Yu, R. Du, G. Fan, Y. Liu, Z. Liu, J. Xiang, Y. Wang, B. Song, X. Gu, L. Guan, Y. Wei, H. Li, X. Wu, J. Xu, S. Tu, Y. Zhang, H. Chen, B. Cao, Clinical course and risk factors for mortality of adult inpatients with COVID-19 in Wuhan, China: a retrospective cohort study, *Lancet* 395 (2020) 1054–1062, [https://doi.org/10.1016/S0140-6736\(20\)30566-3](https://doi.org/10.1016/S0140-6736(20)30566-3).
- [131] R.A. Seaton, C.L. Gibbons, L. Cooper, W. Malcolm, R. McKinney, S. Dundas, D. Griffith, D. Jeffreys, K. Hamilton, B. Choo-Kang, S. Brittain, D. Guthrie, J. Sneddon, Survey of antibiotic and antifungal prescribing in patients with suspected and confirmed COVID-19 in Scottish hospitals, *J. Infect.* 81 (2020) 952–960, <https://doi.org/10.1016/j.jinf.2020.09.024>.
- [132] G. Zhang, C. Zhang, J. Liu, Y. Zhang, W. Fu, Occurrence, fate, and risk assessment of antibiotics in conventional and advanced drinking water treatment systems: From source to tap, *J. Environ. Manag.* 358 (2024) 120746, <https://doi.org/10.1016/j.jenvman.2024.120746>.
- [133] G. Mascolo, L. Balest, D. Cassano, G. Laera, A. Lopez, A. Pollice, C. Salerno, Biodegradability of pharmaceutical industrial wastewater and formation of recalcitrant organic compounds during aerobic biological treatment, *Bioresour. Technol.* 101 (2010) 2585–2591, <https://doi.org/10.1016/j.biortech.2009.10.057>.
- [134] D.L. McCurry, S.E. Bear, J. Bae, D.L. Sedlak, P.L. McCarty, W.A. Mitch, Superior removal of disinfection byproduct precursors and pharmaceuticals from wastewater in a staged anaerobic fluidized membrane bioreactor compared to activated sludge, *Environ. Sci. Technol. Lett.* 1 (2014) 459–464, <https://doi.org/10.1021/ez500279a>.
- [135] G. Mascolo, G. Laera, A. Pollice, D. Cassano, A. Pinto, C. Salerno, A. Lopez, Effective organics degradation from pharmaceutical wastewater by an integrated process including membrane bioreactor and ozonation, *Chemosphere* 78 (2010) 1100–1109, <https://doi.org/10.1016/j.chemosphere.2009.12.042>.
- [136] Z. Guo, H. He, G. Yang, K. Liu, Y. Xi, Z. Li, Y. Luo, Z. Liao, G. Dao, X. Ren, B. Huang, X. Pan, The environmental risks of antiviral drug arbidol in eutrophic lake: interactions with *Microcystis aeruginosa*, *J. Hazard. Mater.* 466 (2024) 133609, <https://doi.org/10.1016/j.jhazmat.2024.133609>.
- [137] M. Lindroos, D. Hörnström, G. Larsson, M. Gustavsson, A.J.A. van Maris, Continuous removal of the model pharmaceutical chloroquine from water using melanin-covered *Escherichia coli* in a membrane bioreactor, *J. Hazard. Mater.* 365 (2019) 74–80, <https://doi.org/10.1016/j.jhazmat.2018.10.081>.
- [138] Y. Xu, Y. Liu, C. Liang, W. Guo, H.H. Ngo, L. Peng, Favipiravir biotransformation by a side-stream partial nitrification sludge: transformation mechanisms, pathways and toxicity evaluation, *Chemosphere* 353 (2024) 141580, <https://doi.org/10.1016/j.chemosphere.2024.141580>.
- [139] L. Zhao, Y. Li, Z. Gan, W. Sun, S. Su, Z. Li, L. Shi, Distribution, fate and removal efficiency of anthelmintic drugs in wastewater treatment plants, *Sci. Total Environ.* 908 (2024) 168240, <https://doi.org/10.1016/j.scitotenv.2023.168240>.
- [140] M. Bayati, T.L. Ho, D.C. Vu, F. Wang, E. Rogers, C. Cuvellier, S. Huebotter, E. C. Inniss, R. Udawatta, S. Jose, C.-H. Lin, Assessing the efficiency of constructed wetlands in removing PPCPs from treated wastewater and mitigating the ecotoxicological impacts, *Int. J. Hyg. Environ. Health* 231 (2021), <https://doi.org/10.1016/j.ijheh.2020.113664>.
- [141] L. Sbardella, J. Comas, A. Fenu, I. Rodriguez-Roda, M. Weemaes, Advanced biological activated carbon filter for removing pharmaceutically active compounds from treated wastewater, *Sci. Total Environ.* 636 (2018) 519–529, <https://doi.org/10.1016/j.scitotenv.2018.04.214>.
- [142] Q.M. Zeeshan, S. Qiu, J. Gu, A.-W. Abbew, Z. Wu, Z. Chen, S. Xu, S. Ge, Unravelling multiple removal pathways of oseltamivir in wastewater by microalgae through experimentation and computation, *J. Hazard. Mater.* 427 (2022) 128139, <https://doi.org/10.1016/j.jhazmat.2021.128139>.
- [143] H. Matsuo, H. Sakamoto, K. Arizono, R. Shinohara, Behavior of pharmaceuticals in waste water treatment plant in Japan, *Bull. Environ. Contam. Toxicol.* 87 (2011) 31–35, <https://doi.org/10.1007/s00128-011-0299-7>.
- [144] S. Mohammadi, G. Moussavi, K. Kiyannmehr, S. Shekoohiyan, M. Heidari, K. Naddafi, S. Giannakis, Degradation of the antiviral remdesivir by a novel, continuous-flow, helical-baffle incorporating VUV/UVC photoreactor: performance assessment and enhancement by inorganic peroxides, *Sep. Purif. Technol.* 298 (2022) 121665, <https://doi.org/10.1016/j.seppur.2022.121665>.
- [145] Q. Liu, X. Feng, N. Chen, F. Shen, H. Zhang, S. Wang, Z. Sheng, J. Li, Occurrence and risk assessment of typical PPCPs and biodegradation pathway of ribavirin in wastewater treatment plants, *Environ. Sci. Ecotechnol.* 11 (2022) 100184, <https://doi.org/10.1016/j.ese.2022.100184>.
- [146] Y. Liu, C. Gao, L. Liu, H. Wang, Green degradation for ribavirin on sulfur-doped MnFe₂O₄ photoelectrocatalysis cathode electrode, *Sep. Purif. Technol.* 326 (2023) 124833, <https://doi.org/10.1016/j.seppur.2023.124833>.
- [147] C. Muriuki, P. Kairigo, P. Home, E. Ngumba, J. Raude, A. Gachanja, T. Tuhkanen, Mass loading, distribution, and removal of antibiotics and antiretroviral drugs in selected wastewater treatment plants in Kenya, *Sci. Total Environ.* 743 (2020) 140655, <https://doi.org/10.1016/j.scitotenv.2020.140655>.
- [148] T.A. Heinrich, R.S. da Silva, K.M. Miranda, C.H. Switzer, D.A. Wink, J.M. Fukuto, Biological nitric oxide signalling: chemistry and terminology, *Br. J. Pharmacol.* 169 (2013) 1417–1429, <https://doi.org/10.1111/bph.12217>.
- [149] E. Fernandez-Fontaina, F. Omil, J.M. Lema, M. Carballa, Influence of nitrifying conditions on the biodegradation and sorption of emerging micropollutants, *Water Res.* 46 (2012) 5434–5444, <https://doi.org/10.1016/j.watres.2012.07.037>.
- [150] V. Osorio, A. Cruz-Alcalde, S. Pérez, Nitrosation and nitration of diclofenac and structurally related nonsteroidal anti-inflammatory drugs (NSAIDs) in nitrifying activated sludge, *Sci. Total Environ.* 807 (2022) 150533, <https://doi.org/10.1016/j.scitotenv.2021.150533>.
- [151] S. Park, S. Oh, Activated sludge-degrading analgesic drug acetaminophen: acclimation, microbial community dynamics, degradation characteristics, and bioaugmentation potential, *Water Res.* 182 (2020) 115957, <https://doi.org/10.1016/j.watres.2020.115957>.
- [152] Z. Liu, Q. Liu, C. Hao, Y. Zhao, Insights into the response mechanisms of activated sludge system under long-term dexamethasone stress, *Sci. Total Environ.* 933 (2024) 173007, <https://doi.org/10.1016/j.scitotenv.2024.173007>.
- [153] Y. Jang, H.-S. Kim, S.-Y. Ham, J.-H. Park, H.-D. Park, Investigation of critical sludge characteristics for membrane fouling in a submerged membrane bioreactor: role of soluble microbial products and extracted extracellular polymeric substances, *Chemosphere* 271 (2021) 129879, <https://doi.org/10.1016/j.chemosphere.2021.129879>.
- [154] D.M. González-Pérez, J.I. Pérez, M.A. Gómez, Behaviour of the main nonsteroidal anti-inflammatory drugs in a membrane bioreactor treating urban wastewater at high hydraulic- and sludge-retention time, *J. Hazard. Mater.* 336 (2017) 128–138, <https://doi.org/10.1016/j.jhazmat.2017.04.059>.
- [155] N. Vieno, M. Sillanpää, Fate of diclofenac in municipal wastewater treatment plant — a review, *Environ. Int.* 69 (2014) 28–39, <https://doi.org/10.1016/j.envint.2014.03.021>.
- [156] T. Trinh, B. van den Akker, H.M. Coleman, R.M. Stuetz, J.E. Drewes, P. Le-Clech, S.J. Khan, Seasonal variations in fate and removal of trace organic chemical contaminants while operating a full-scale membrane bioreactor, *Sci. Total Environ.* 550 (2016) 176–183, <https://doi.org/10.1016/j.scitotenv.2015.12.083>.
- [157] M. Gutierrez, D. Mutavdžić Pavlović, D. Stipančević, S. Repec, F. Avolio, M. Zanella, P. Verlicchi, A thorough analysis of the occurrence, removal and environmental risks of organic micropollutants in a full-scale hybrid membrane bioreactor fed by hospital wastewater, *Sci. Total Environ.* 914 (2024) 169848, <https://doi.org/10.1016/j.scitotenv.2023.169848>.
- [158] W. Liu, X. Song, X. Ding, R. Xia, X. Lin, G. Li, L.D. Nghiem, W. Luo, Antibiotic removal from swine farming wastewater by anaerobic membrane bioreactor: role of hydraulic retention time, *J. Membr. Sci.* 677 (2023) 121629, <https://doi.org/10.1016/j.memsci.2023.121629>.
- [159] W. Shu, Y. Zhang, D. Wen, Q. Wu, H. Liu, M.-h Cui, B. Fu, J. Zhang, Y. Yao, Anaerobic biodegradation of levofloxacin by enriched microbial consortia: effect of electron acceptors and carbon source, *J. Hazard. Mater.* 414 (2021) 125520, <https://doi.org/10.1016/j.jhazmat.2021.125520>.
- [160] S. Wang, R. Yuan, H. Chen, F. Wang, B. Zhou, Anaerobic biodegradation of four sulfanilamide antibiotics: kinetics, pathways and microbiological studies, *J. Hazard. Mater.* 416 (2021) 125840, <https://doi.org/10.1016/j.jhazmat.2021.125840>.
- [161] A.C. Reis, B.A. Kolvenbach, O.C. Nunes, P.F.X. Corvini, Biodegradation of antibiotics: the new resistance determinants – part I, *N. Biotechnol.* 54 (2020) 34–51, <https://doi.org/10.1016/j.nbt.2019.08.002>.
- [162] Q. Zhao, W. Guo, H. Luo, C. Xing, H. Wang, B. Liu, Q. Si, D. Li, L. Sun, N. Ren, Insights into removal of sulfonamides in anaerobic activated sludge system: mechanisms, degradation pathways and stress responses, *J. Hazard. Mater.* 423 (2022) 127248, <https://doi.org/10.1016/j.jhazmat.2021.127248>.
- [163] S. Arriaga, N. de Jonge, M.L. Nielsen, H.R. Andersen, V. Borregaard, K. Jewel, T. A. Ternes, J.L. Nielsen, Evaluation of a membrane bioreactor system as post-treatment in waste water treatment for better removal of micropollutants, *Water Res.* 107 (2016) 37–46, <https://doi.org/10.1016/j.watres.2016.10.046>.

- [164] K.C. Wijekoon, J.A. McDonald, S.J. Khan, F.I. Hai, W.E. Price, L.D. Nghiem, Development of a predictive framework to assess the removal of trace organic chemicals by anaerobic membrane bioreactor, *Bioresour. Technol.* 189 (2015) 391–398, <https://doi.org/10.1016/j.biortech.2015.04.034>.
- [165] W. Liu, X. Song, N. Huda, M. Xie, G. Li, W. Luo, Comparison between aerobic and anaerobic membrane bioreactors for trace organic contaminant removal in wastewater treatment, *Environ. Technol. Innov.* 17 (2020) 100564, <https://doi.org/10.1016/j.eti.2019.100564>.
- [166] S.V. Mohan, S.V. Raghavulu, D. Peri, P.N. Sarma, Integrated function of microbial fuel cell (MFC) as bio-electrochemical treatment system associated with bioelectricity generation under higher substrate load, *Biosens. Bioelectron.* 24 (2009) 2021–2027, <https://doi.org/10.1016/j.bios.2008.10.011>.
- [167] T.S. Utami, R. Arbiandi, I.M. Hidayatullah, F. Yusupandi, M. Hamdan, N. Fadilah Putri, F.A. Riyadi, R. Boopathy, Paracetamol degradation in a dual-chamber rectangular membrane bioreactor using microbial fuel cell system with a microbial consortium from sewage sludge, *Case Stud. Chem. Environ. Eng.* 9 (2024) 100551, <https://doi.org/10.1016/j.csee.2023.100551>.
- [168] J. Jiang, H. Wang, S. Zhang, S. Li, W. Zeng, F. Li, The influence of external resistance on the performance of microbial fuel cell and the removal of sulfamethoxazole wastewater, *Bioresour. Technol.* 336 (2021) 125308, <https://doi.org/10.1016/j.biortech.2021.125308>.
- [169] P. Chen, J. Jiang, S. Zhang, X. Wang, X. Guo, F. Li, Enzymatic response and antibiotic resistance gene regulation by microbial fuel cells to resist sulfamethoxazole, *Chemosphere* 325 (2023) 138410, <https://doi.org/10.1016/j.chemosphere.2023.138410>.
- [170] Y. Liu, C. Gao, L. Liu, H. Wang, T-mode adsorption and photoelectrocatalysis degradation for acyclovir on CuMn2O4/WO3/g-C3N4 electrode, *Chem. Eng. J.* 464 (2023) 142577, <https://doi.org/10.1016/j.cej.2023.142577>.
- [171] T. An, J. An, Y. Gao, G. Li, H. Fang, W. Song, Photocatalytic degradation and mineralization mechanism and toxicity assessment of antiviral drug acyclovir: experimental and theoretical studies, *Appl. Catal. B: Environ.* 164 (2015) 279–287, <https://doi.org/10.1016/j.apcatb.2014.09.009>.
- [172] S. Jain, P. Kumar, R.K. Vyas, P. Pandit, A.K. Dalai, Adsorption optimization of acyclovir on prepared activated carbon, *Can. J. Chem. Eng.* 92 (2014) 1627–1635, <https://doi.org/10.1002/cjce.22026>.
- [173] X. Qu, H. Zeng, Y. Gao, D. Xu, Phosphate enhanced thermal activation of peroxymonosulfate for acyclovir removal: process comparison and DFT calculation, *J. Environ. Chem. Eng.* 11 (2023) 111525, <https://doi.org/10.1016/j.jece.2023.111525>.
- [174] T. Zhang, G. Bai, N. Cai, Y. Lei, P. Guo, J. Xu, The carbon-doped Fe3O4 montmorillonite particle electrode for the degradation of antiviral drugs in electro-Fenton system, *Appl. Clay Sci.* 243 (2023) 107056, <https://doi.org/10.1016/j.clay.2023.107056>.
- [175] Y. Li, L. Zhao, D. Chen, T. Sen, G. Lu, J. Liu, X. Du, P. Sun, Y. Yang, Specific adsorption of antiviral drugs on ionic liquid-modified metal-organic framework: adsorption behavior, mechanism, and DFT analysis, *Chem. Eng. J.* 497 (2024) 155070, <https://doi.org/10.1016/j.cej.2024.155070>.
- [176] S. Midassi, A. Bedoui, N. Bensalah, Efficient degradation of chloroquine drug by electro-Fenton oxidation: effects of operating conditions and degradation mechanism, *Chemosphere* 260 (2020), <https://doi.org/10.1016/j.chemosphere.2020.127558>.
- [177] H. Dai, W. Luo, L. Jin, L. Deng, Q. Wang, J. Hu, R.P. Singh, Degradation of chloroquine phosphate during UV/H2O2 process: performance, kinetics, and degradation pathways, *J. Environ. Chem. Eng.* 12 (2024) 112493, <https://doi.org/10.1016/j.jece.2024.112493>.
- [178] F. Dong, J. Li, Q. Lin, D. Wang, C. Li, Y. Shen, T. Zeng, S. Song, Oxidation of chloroquine drug by ferrate: kinetics, reaction mechanism and antibacterial activity, *Chem. Eng. J.* 428 (2022) 131408, <https://doi.org/10.1016/j.cej.2021.131408>.
- [179] X.-X. Wang, L. Liu, Q.-F. Li, H. Xiao, M.-L. Wang, H.-C. Tu, J.-M. Lin, R.-S. Zhao, Nitrogen-rich based conjugated microporous polymers for highly efficient adsorption and removal of COVID-19 antiviral drug chloroquine phosphate from environmental waters, *Sep. Purif. Technol.* 305 (2023) 122517, <https://doi.org/10.1016/j.seppur.2022.122517>.
- [180] P. Ashrafi, D. Nematollahi, A. Shabanloo, A. Ansari, A. Sadatnabi, A. Sadeghinia, Enhanced favipiravir drug degradation using the synergy of PbO2-based anodic oxidation and Fe-MOF-based cathodic electro-Fenton, *Environ. Res.* 262 (2024) 119883, <https://doi.org/10.1016/j.envres.2024.119883>.
- [181] S.-T. Huang, Y.-Q. Lei, P.-R. Guo, H.-X. Chen, S.-C. Gan, Z.-H. Diao, Electrocatalytic degradation of Favipiravir by heteroatom (P and S) doped biomass-derived carbon with high oxygen reduction reaction activity, *Chem. Eng. J.* 484 (2024) 149543, <https://doi.org/10.1016/j.cej.2024.149543>.
- [182] B.I. Olu-Owolabi, P.N. Diagbaya, F.M. Mtunzi, R.-A. Düring, Utilizing eco-friendly kaolinite-biochar composite adsorbent for removal of ivermectin in aqueous media, *J. Environ. Manag.* 279 (2021) 111619, <https://doi.org/10.1016/j.jenvman.2020.111619>.
- [183] S. Patibandla, J.-Q. Jiang, X. Shu, Toxicity assessment of four pharmaceuticals in aquatic environment before and after ferrate(VI) treatment, *J. Environ. Chem. Eng.* 6 (2018) 3787–3797, <https://doi.org/10.1016/j.jece.2018.05.024>.
- [184] S. Saghir, Z. Xiao, Synergistic approach for synthesis of functionalized biochar for efficient adsorption of Lopinavir from polluted water, *Bioresour. Technol.* 391 (2024) 129916, <https://doi.org/10.1016/j.biortech.2023.129916>.
- [185] M. Hojamberdiev, B. Czech, A. Wasilewska, A. Boguszewska-Czubarra, K. Yubuta, H. Wagata, S.S. Daminova, Z.C. Kadirova, R. Vargas, Detoxifying SARS-CoV-2 antiviral drugs from model and real wastewaters by industrial waste-derived multiphase photocatalysts, *J. Hazard. Mater.* 429 (2022) 128300, <https://doi.org/10.1016/j.jhazmat.2022.128300>.
- [186] A. Demir, N. Oturan, B. Özyurt, C. Trellu, M.A. Oturan, Degradation of antiviral drug molnupiravir using a dual function Fe/FeIII/LDH@carbon felt cathode in the heterogeneous electro-Fenton process: kinetics and mineralization study, *J. Environ. Chem. Eng.* 12 (2024) 113665, <https://doi.org/10.1016/j.jece.2024.113665>.
- [187] L. Tabana, D.-R. Booyens, S. Tichapondwa, Photocatalytic degradation of efavirenz and nevirapine using visible light-activated Ag-AgBr-LDH nanocomposite catalyst, *J. Photochem. Photobiol. A: Chem.* 444 (2023) 114997, <https://doi.org/10.1016/j.jphotochem.2023.114997>.
- [188] Y.A. Bhembe, L.P. Lukhele, L. Hlekelele, S.S. Ray, A. Sharma, D.-V.N. Vo, L. N. Dlamini, Photocatalytic degradation of nevirapine with a heterostructure of few-layer black phosphorus coupled with niobium (V) oxide nanoflowers (FL-BP@Nb2O5), *Chemosphere* 261 (2020) 128159, <https://doi.org/10.1016/j.chemosphere.2020.128159>.
- [189] P.N. Kunene, P.N. Mahlambi, T. Ndlovu, Adsorption of antiretroviral drugs, abacavir, nevirapine, and efavirenz from river water and wastewater using exfoliated graphite: isotherm and kinetic studies, *J. Environ. Manag.* 360 (2024) 121200, <https://doi.org/10.1016/j.jenvman.2024.121200>.
- [190] H. Mestankova, K. Schirmer, B.I. Escher, U. von Gunten, S. Canonica, Removal of the antiviral agent oseltamivir and its biological activity by oxidative processes, *Environ. Pollut.* 161 (2012) 30–35, <https://doi.org/10.1016/j.envpol.2011.09.018>.
- [191] M. Hosseini, H. Rasoulzadeh, H. Akbari, H. Akbari, A. Adibzadeh, Photoelectrocatalytic degradation of remdesivir from aqueous solutions using Ni-doped ZnO nanocomposite: kinetic, degradation pathway, toxicity reduction and reusability, *J. Photochem. Photobiol. A: Chem.* 450 (2024) 115416, <https://doi.org/10.1016/j.jphotochem.2023.115416>.
- [192] A. Babamir Satehi, M. Anbia, F. Yazdi, Green synthesis of magnetic graphene-like biochar with oxygen vacancies for efficient adsorption and degradation of emerging antivirals from water, *J. Alloy. Compd.* 1007 (2024) 176366, <https://doi.org/10.1016/j.jallcom.2024.176366>.
- [193] T. Huang, J. Guo, G. Lu, Ultraviolet-coupled advanced oxidation processes for anti-COVID-19 drugs treatment: degradation mechanisms, transformation products and toxicity evolution, *Chemosphere* 303 (2022) 134968, <https://doi.org/10.1016/j.chemosphere.2022.134968>.
- [194] S. Ostovar, G. Moussavi, S. Mohammadi, M.L. Marin, F. Bosca, A. Diego-Lopez, S. Giannakis, Developing a novel Ti-doped γAl2O3 xerogel with high photocatalytic chemical and microbial removal performance: Characterization and mechanistic insights, *Chem. Eng. J.* 464 (2023) 142545, <https://doi.org/10.1016/j.cej.2023.142545>.
- [195] X. Liu, Y. Hong, S. Ding, W. Jin, S. Dong, R. Xiao, W. Chu, Transformation of antiviral ribavirin during ozone/PMS intensified disinfection amid COVID-19 pandemic, *Sci. Total Environ.* 790 (2021) 148030, <https://doi.org/10.1016/j.scitotenv.2021.148030>.
- [196] Z. Li, Q. Zheng, K. Cai, L. Yang, J. Yang, H. Sun, C. Liu, W. Zhang, Y. Zheng, C. Wu, Degradation of ribavirin by potassium ferrate(VI): kinetics, degradation pathway and toxicity assessment, *Process Saf. Environ. Prot.* 180 (2023) 735–743, <https://doi.org/10.1016/j.psep.2023.10.034>.
- [197] J. Jiang, Z. An, M. Li, Y. Huo, Y. Zhou, J. Xie, M. He, Comparison of ribavirin degradation in the UV/H2O2 and UV/PDS systems: reaction mechanism, operational parameter and toxicity evaluation, *J. Environ. Chem. Eng.* 11 (2023) 109193, <https://doi.org/10.1016/j.jece.2022.109193>.
- [198] T.G. Kebede, M.B. Seroto, R.C. Chokwe, S. Dube, M.M. Nindi, Adsorption of antiretroviral (ARVs) and related drugs from environmental wastewaters using nanofibers, *J. Environ. Chem. Eng.* 8 (2020) 104049, <https://doi.org/10.1016/j.jece.2020.104049>.
- [199] B.O. Ojo, O.A. Arotiba, N. Mabuba, Evaluation of FTO-BaTiO3/NiTiO3 electrode towards sonoelectrochemical degradation of emerging pharmaceutical contaminants in water, *Colloids Surf. A: Physicochem. Eng. Asp.* 647 (2022) 129201, <https://doi.org/10.1016/j.colsurfa.2022.129201>.
- [200] V.K. Sharma, L. Chen, R. Zboril, Review on high valent Fe(VI) (Ferrate): a sustainable green oxidant in organic chemistry and transformation of pharmaceuticals, *ACS Sustain. Chem. Eng.* 4 (2016) 18–34, <https://doi.org/10.1021/acssuschemeng.5b01202>.
- [201] J.-Y. Cao, Y. Du, X. Dai, T. Liu, Z.-J. Wang, J. Li, H. Zhang, P. Zhou, B. Lai, Ferrate (VI)-based synergistic oxidation processes (Fe(VI)-SOPs): promoted reactive species production, micropollutant/microorganism elimination, and toxicity reduction, *Chem. Eng. J.* 489 (2024), <https://doi.org/10.1016/j.cej.2024.151180>.
- [202] X.-S. Wang, C.-N. Ma, Y.-L. Liu, G.-J. Wang, B. Tang, H. Song, Z. Gao, J. Ma, L. Wang, High efficiency removal of organic and inorganic iodine with ferrate Fe (VI) through oxidation and adsorption, *Water Res.* 246 (2023), <https://doi.org/10.1016/j.watres.2023.120671>.
- [203] B. Suyamud, J. Lohwacharin, Y. Yang, V.K. Sharma, Antibiotic resistant bacteria and genes in shrimp aquaculture water: identification and removal by ferrate(VI), *J. Hazard. Mater.* 420 (2021) 126572, <https://doi.org/10.1016/j.jhazmat.2021.126572>.
- [204] C. Li, X.Z. Li, N. Graham, N.Y. Gao, The aqueous degradation of bisphenol A and steroid estrogens by ferrate, *Water Res.* 42 (2008) 109–120, <https://doi.org/10.1016/j.watres.2007.07.023>.
- [205] H. Wang, Y. Liu, J.-Q. Jiang, Reaction kinetics and oxidation product formation in the degradation of acetaminophen by ferrate (VI), *Chemosphere* 155 (2016) 583–590, <https://doi.org/10.1016/j.chemosphere.2016.04.088>.

- [206] Z. Li, Q. Zheng, K. Cai, L. Yang, J. Yang, H. Sun, C. Liu, W. Zhang, Y. Zheng, C. Wu, Degradation of ribavirin by potassium ferrate(VI): kinetics, degradation pathway and toxicity assessment, *Process Saf. Environ. Prot.* 180 (2023) 735–743, <https://doi.org/10.1016/j.psep.2023.10.034>.
- [207] Z. Li, C. Wu, Q. Zheng, J. Yang, L. Yang, H. Sun, C. Liu, W. Zhang, Y. Zheng, K. Cai, Accelerated degradation and toxicity reduction of ribavirin by organic free radicals in the ferrate-acetylacetonate system, *Sep. Purif. Technol.* 330 (2024), <https://doi.org/10.1016/j.seppur.2023.125636>.
- [208] C. Jing, W. Yibo, Z. Yaxue, Z. Wenjuan, Z. Rui, W. Zhe, W. Shaopo, Oxidation of ibuprofen in water by UV/O₃ process: removal, byproducts, and degradation pathways, *J. Water Process Eng.* 53 (2023) 103721, <https://doi.org/10.1016/j.jwpe.2023.103721>.
- [209] W.-j. Hu, L. Chang, Y. Yang, X. Wang, Y.-c. Xie, J.-s. Shen, B. Tan, J. Liu, Pharmacokinetics and tissue distribution of remdesivir and its metabolites nucleotide monophosphate, nucleotide triphosphate, and nucleoside in mice, *Acta Pharmacol. Sin.* 42 (2021) 1195–1200, <https://doi.org/10.1038/s41401-020-00537-9>.
- [210] H. Pourzamani, Y. Hajizadeh, N. Mengelizadeh, Application of three-dimensional electrofenton process using MWCNTs-Fe₃O₄ nanocomposite for removal of diclofenac, *Process Saf. Environ. Prot.* 119 (2018) 271–284, <https://doi.org/10.1016/j.psep.2018.08.014>.
- [211] C. Zhou, Y. Wang, J. Chen, L. Xu, H. Huang, J. Niu, High-efficiency electrochemical degradation of antiviral drug abacavir using a penetration flux porous Ti/SnO₂-Sb anode, *Chemosphere* 225 (2019) 304–310, <https://doi.org/10.1016/j.chemosphere.2019.03.036>.
- [212] H. Zhang, Q. Zhao, K. Zhong, R. Bai, J. Dong, J. Ma, J. Zhang, T.J. Strathmann, Overlooked interaction between redox-mediator and bisphenol-A in permanganate oxidation, *Environ. Sci. Ecotechnology* 21 (2024) 100421, <https://doi.org/10.1016/j.ese.2024.100421>.
- [213] J. Jiang, S.-Y. Pang, J. Ma, Oxidation of triclosan by permanganate (Mn(VII)): importance of ligands and in situ formed manganese oxides, *Environ. Sci. Technol.* 43 (2009) 8326–8331, <https://doi.org/10.1021/es901663d>.
- [214] T. Rodríguez-Álvarez, R. Rodil, J.B. Quintana, S. Triñanes, R. Cela, Oxidation of non-steroidal anti-inflammatory drugs with aqueous permanganate, *Water Res.* 47 (2013) 3220–3230, <https://doi.org/10.1016/j.watres.2013.03.034>.
- [215] Y. Zhou, Y. Gao, J. Jiang, Y.-M. Shen, S.-Y. Pang, Y. Song, Q. Guo, A comparison study of levofloxacin degradation by peroxymonosulfate and permanganate: kinetics, products and effect of quinone group, *J. Hazard. Mater.* 403 (2021) 123834, <https://doi.org/10.1016/j.jhazmat.2020.123834>.
- [216] S.M. Tuwar, R.M. Hanabaratti, Kinetics and mechanistic investigations on antiviral drug-valacyclovir hydrochloride by heptavalent alkaline permanganate, *J. Chem. Sci.* 133 (2021), <https://doi.org/10.1007/s12039-021-01969-4>.
- [217] Y. Feng, Y. Tao, Q. Meng, J. Qu, S. Ma, S. Han, Y. Zhang, Microwave-combined advanced oxidation for organic pollutants in the environmental remediation: an overview of influence, mechanism, and prospective, *Chem. Eng. J.* 441 (2022) 135924, <https://doi.org/10.1016/j.cej.2022.135924>.
- [218] N.M. Mahmoodi, S. Keshavarzi, M. Ghezlbash, Synthesis of nanoparticle and modelling of its photocatalytic dye degradation ability from colored wastewater, *J. Environ. Chem. Eng.* 5 (2017) 3684–3689, <https://doi.org/10.1016/j.jece.2017.07.010>.
- [219] M. Woche, N. Scheibe, W. von Tümpling, M. Schwidder, Degradation of the antiviral drug zanamivir in wastewater – the potential of a photocatalytic treatment process, *Chem. Eng. J.* 287 (2016) 674–679, <https://doi.org/10.1016/j.cej.2015.11.047>.
- [220] T. Wang, M. Li, W. Wang, X. Liu, X. Qi, X. Su, D. Shi, H. Zhan, Y. Wang, Preparation of TiO₂(B)/GO/ZIF-8 with enhanced photocatalytic performance for degradation ibuprofen under visible light, *Mater. Sci. Eng.: B* 301 (2024) 117163, <https://doi.org/10.1016/j.mseb.2023.117163>.
- [221] M. Mousavi, J.B. Ghasemi, Novel visible-light-responsive Black-TiO₂/CoTiO₃ Z-scheme heterojunction photocatalyst with efficient photocatalytic performance for the degradation of different organic dyes and tetracycline, *J. Taiwan Inst. Chem. Eng.* 121 (2021) 168–183, <https://doi.org/10.1016/j.jtice.2021.04.009>.
- [222] C. Prasse, J. Wenk, J.T. Jasper, T.A. Ternes, D.L. Sedlak, Co-occurrence of photochemical and microbiological transformation processes in open-water unit process wetlands, *Environ. Sci. Technol.* 49 (2015) 14136–14145, <https://doi.org/10.1021/acs.est.5b03783>.
- [223] L. Shi, Y. Shi, Y. Xu, J. Cao, Y. Meng, H. Chen, Metal-organic framework membranes with varying metal ions for enhanced water and wastewater treatment: a critical review, *J. Environ. Chem. Eng.* 11 (2023) 111468, <https://doi.org/10.1016/j.jece.2023.111468>.
- [224] H. Viltres, V. Phung, N. Gupta, C. Morera-Boado, A.M. Sheikhlhar, A. R. Rajabzadeh, S. Srinivasan, Rapid and effective antibiotics elimination from water by Fe-BTB MOF: an insight into adsorption mechanism, *J. Mol. Liq.* 397 (2024), <https://doi.org/10.1016/j.molliq.2024.124105>.
- [225] H. Viltres, V. Phung, N. Gupta, C. Morera-Boado, A. Mohammadi Sheikhlhar, A. Reza Rajabzadeh, S. Srinivasan, Rapid and effective antibiotics elimination from water by Fe-BTB MOF: an insight into adsorption mechanism, *J. Mol. Liq.* 397 (2024) 124105, <https://doi.org/10.1016/j.molliq.2024.124105>.
- [226] X. Mi, R. Ma, X. Pu, X. Fu, M. Geng, J. Qian, FeNi-layered double hydroxide (LDH) @biochar composite for, activation of peroxymonosulfate (PMS) towards enhanced degradation of doxycycline (DOX): characterizations of the catalysts, catalytic performances, degradation pathways and mechanisms, *J. Clean. Prod.* 378 (2022) 134514, <https://doi.org/10.1016/j.jclepro.2022.134514>.
- [227] X.-p Guo, Y. Yang, D.-p Lu, Z.-s Niu, J.-n Feng, Y.-r Chen, F.-y Tou, E. Garner, J. Xu, M. Liu, M.F. Hochella, Biofilms as a sink for antibiotic resistance genes (ARGs) in the Yangtze Estuary, *Water Res.* 129 (2018) 277–286, <https://doi.org/10.1016/j.watres.2017.11.029>.